

THERMAL ANALYSIS OF PULSE
DETONATION ENGINES

by

RAGHU RAMAN GHANDIKOTA

Presented to the Faculty of the Graduate School of
The University of Texas at Arlington in Partial Fulfillment
of the Requirements
for the Degree of

MASTER OF SCIENCE IN AEROSPACE ENGINEERING

THE UNIVERSITY OF TEXAS AT ARLINGTON

DECEMBER 2008

ACKNOWLEDGEMENTS

I would like to take this opportunity to acknowledge the efforts and support of the following people who have helped me in the successful completion of my Master's thesis. First, I would like to thank my supervising professor, Dr. Donald Wilson, Professor and chair, Department of Mechanical Engineering, my mentor in the pursuit of my Master's degree. I am grateful for his esteemed efforts and guidance which have ultimately helped me reach this milestone in my life. He gave me the opportunity of working in the Aerodynamics Research Center and ultimately made me familiar with the concept of the pulse detonation engine. The concepts taught by him in air breathing propulsion and hypersonic air breathing propulsion paved the way to better understand my thesis topic. Secondly I would like to thank Dr Haji Sheik for this valuable suggestion in the area of heat transfer. In spite of being busy, he was always available for help in giving me valuable suggestions in my thesis topic and Dr Zhen Xue Han for his support and encouragement all through my masters program and with whom I enjoyed working with as a Teaching Assistant. I would also like to thank Dr Frank Lu, Director of Aerodynamics Research Center for providing me assistantship all through my Master's program.

I would also like to thank my father Ghandikota Murthy, my mother Vijayalakshmi and my brother Ravi for their love and affection all through my life.

November 20, 2008

ABSTRACT

THERMAL ANALYSIS OF PULSE DETONATION ENGINES

RAGHU RAMAN GHANDIKOTA, MS

The University of Texas at Arlington, 2008

Supervising Professor: Dr. Donald Wilson

The pulse detonation engine (PDE) is a compact system that can be modeled thermodynamically by the Humphrey cycle and is capable of high efficiency. The rapid heat release for stoichiometric fuel/oxidizer ratios results in developing high temperatures. The high temperatures produced during its operation can cause the engine to fail. Thus, operating this engine for a longer duration would become dubious if the temperatures are not dissipated from it. The current research aims to perform a preliminary thermal analysis. This analysis consists of two steps. The first step is to determine the heat dissipated from the engine using the unsteady state analysis, and the second step is to develop a preliminary heat exchanger design. A design method is developed and an example design of a heat exchanger is proposed.

TABLE OF CONTENTS

| | |
|---|------|
| ACKNOWLEDGEMENTS | ii |
| ABSTRACT | iii |
| LIST OF ILLUSTRATIONS | viii |
| LIST OF TABLES | x |
| LIST OF SYMBOLS | xi |
| Chapter | |
| 1. INTRODUCTION | 1 |
| 1.1 Pulse Detonation Engine..... | 1 |
| 1.1.1 Filling Process..... | 3 |
| 1.1.2 CJ Detonation Process | 4 |
| 1.1.3 Taylor Rarefaction Process..... | 5 |
| 1.1.4 Reflected Rarefaction and Exhaust Process..... | 6 |
| 1.1.5 Purging Process..... | 7 |
| 1.2 Objective Of Current Research | 8 |
| 1.3 Chemical Equilibrium Applications..... | 8 |
| 1.4 Energy Analysis of Unsteady-Flow Processes..... | 9 |
| 2. DETERMINATION OF THERMODYNAMIC PROPERTIES USING CHEMICAL EQUILIBRIUM APPLICATIONS CODE..... | 11 |
| 2.1 Input to the CEA Code..... | 11 |

| | |
|--|----|
| 2.2 Output from the CEA Code | 14 |
| 3. AVERAGE THERMODYNAMIC PROPERTIES FOR ONE CYCLE..... | 15 |
| 3.1 Filling Process..... | 15 |
| 3.2 CJ Detonation Process | 15 |
| 3.3 Taylor Rarefaction Wave Process..... | 17 |
| 3.3.1 Front Boundary Conditions of Taylor Rarefaction Wave..... | 17 |
| 3.3.2 End Wall Conditions of Taylor Rarefaction Wave..... | 19 |
| 3.3.3 Average Conditions of Flow During Detonation Process..... | 21 |
| 3.4 Reflected Rarefaction Process | 23 |
| 3.4.1 Initial Conditions of Reflection Process | 23 |
| 3.4.2 Final Conditions of Reflection Process..... | 25 |
| 3.4.3 Average Conditions of Flow During Reflection Process..... | 27 |
| 3.5 Blow Down Process | 27 |
| 3.5.1 Initial Conditions of Blow Down Process..... | 27 |
| 3.5.2 Final Conditions of Blow Down Process..... | 28 |
| 3.5.3 Average Conditions of Flow During Blow Down Process..... | 30 |
| 3.6 Purging Process..... | 30 |
| 3.6.1 Initial Conditions of Purging Process | 31 |
| 3.6.2 Final Conditions of Purging Process..... | 31 |
| 4. CALCULATION OF HEAT DISSIPATED FOR ONE CYCLE OF OPERATION..... | 35 |

| | |
|---|--------|
| 4.1 Application of Energy Expression to The Pulse Detonation Engine | 35 |
| 4.1.1 Filling Process..... | 36 |
| 4.1.2 CJ Detonation Process | 38 |
| 4.1.3 Taylor Rarefaction Wave Process..... | 40 |
| 4.1.4 Reflected Rarefaction Wave Process | 42 |
| 4.1.5 Blow Down Process..... | 45 |
| 4.1.6 Purging Process..... | 46 |
| 5. CALCULATION OF WALL TEMPERATURES USING GREEN’S FUNCTIONS..... | 49 |
| 5.1 Transient Analysis Solution of Heat Conduction Through Hollow Cylinders..... | 50 |
| 5.2 Calculation of Wall Temperatures for One Cycle of Operation | 55 |
| 5.2.1 Wall Temperatures During Filling Process..... | 56 |
| 5.2.2 Wall Temperatures During CJ Detonation Process | 57 |
| 5.2.3 Wall Temperatures During Taylor Rarefaction Wave Process..... | 58 |
| 5.2.4 Wall Temperatures During Reflected Rarefaction Wave Process | 58 |
| 5.2.5 Wall Temperatures During Blow Down Process..... | 59 |
| 5.2.6 Wall Temperatures During Purging Process..... | 59 |
| 5.3 Comparison of Copper and Steel Metals | 61 |
| 5.4 Comparison of Transient Analysis with Steady State Analysis..... | 63 |

| | |
|---|----|
| 5.4.1 Steady State Heat Conduction Relations | 63 |
| 5.4.2 Steady state values of wall Temperatures | 65 |
| 6. CONCLUSIONS AND RECOMMENDATIONS FOR FUTURE WORK..... | 67 |
| 6.1 Conclusions..... | 67 |
| 6.2 Recommendations for Future Work..... | 68 |
| REFERENCES..... | 70 |
| BIOGRAPHICAL INFORMATION..... | 72 |

LIST OF ILLUSTRATIONS

| FIGURE | Page |
|---|------|
| 1.1 Block Diagram of a Turbojet Engine..... | 2 |
| 1.2 Block Diagram of a Pulse Detonation Engine | 2 |
| 1.3 Schematic of a Pulse Detonation Cycle | 3 |
| 1.4 Cross Section of a Detonation Tube | 4 |
| 1.5 Sectional View of the Detonation Tube..... | 6 |
| 2.1 Input Section of the CEA Code for Hydrogen and Oxygen | 11 |
| 2.2 Fuel Selection Section of the CEA Code..... | 12 |
| 2.3 Oxidizer Selection Section of the Code | 12 |
| 2.4 Type of Detonation Selection Section of the CEA Code..... | 13 |
| 2.5 Execution Section of the CEA CODE | 13 |
| 3.1 Variation of Temperature During Taylor Wave Process | 20 |
| 3.2 Variation of Pressure During Taylor Wave Process | 20 |
| 3.3 Variation of Density During Taylor Wave Process | 21 |
| 3.4 Temperature Variation After Taylor Wave Process | 22 |
| 3.5 Density Variation After Taylor Wave Process | 22 |
| 3.6 Pressure Variation After Taylor Wave Process | 23 |
| 3.7 Variation in Temperature During Reflection Process..... | 25 |

| | |
|---|----|
| 3.8 Variation in Pressure During Reflection Process..... | 26 |
| 3.9 Variation in Density During Reflection Proces | 26 |
| 3.10 Variation in Temperature During Blow Down process | 29 |
| 3.11 Variation in Pressure During Blow Down Process..... | 29 |
| 3.12 Variation in Density During Blow Down Process | 30 |
| 3.13 Pressure Variation for Taylor Wave and Reflection Processes | 32 |
| 3.14 Pressure Variation for Taylor Wave and Reflection Processes | 33 |
| 4.1 Detonation Tube During Filling Process | 36 |
| 4.2 Detonation Tube During Detonation Process | 38 |
| 4.3 Detonation Tube During Taylor Wave Process | 40 |
| 4.4 Detonation Tube During Reflected Rarefaction Process | 42 |
| 4.5 Detonation Tube During Blow Down Process..... | 45 |
| 4.6 Detonation Tube During Purging Process | 46 |
| 5.1 Cross Sectional View of the Detonation Tube..... | 49 |
| 5.2 Temperature Distribution Along the Inner Walls of Detonation Tube (Copper) | 64 |
| 5.3 Temperature Distribution Along the Outer Walls of Detonation Tube (Copper) | 65 |

LIST OF TABLES

| TABLE | Page |
|--|------|
| 2.1 Thermodynamic Properties After CJ Detonation Process (CEA) | 14 |
| 3.1 Average Thermodynamic Properties During Each Process | 34 |
| 4.1 Thermodynamic Properties During the Filling Process | 38 |
| 4.2 Thermodynamic Properties During CJ Detonation Process | 40 |
| 4.3 Thermodynamic Properties During Taylor Rarefaction Wave Process | 42 |
| 4.4 Thermodynamic Properties During Reflected Rarefaction Process | 44 |
| 4.5 Thermodynamic Properties During Blow Down Process | 45 |
| 4.6 Thermodynamic Properties During Purging Process | 48 |
| 5.1 Time period, Temperatures and Heat Dissipated During Each Process | 53 |
| 5.2 Wall Temperatures During Each Process (COPPER)..... | 60 |
| 5.3 Wall Temperatures during Each Process (STEEL) | 62 |

LIST OF SYMBOLS

| | |
|-------------|---|
| A_i | Area of the detonation tube (m^2) |
| B_i | Biot number |
| C | Specific heat of steel |
| C_p | Specific heat at constant pressure $\left(\frac{kJ}{kg.K}\right)$ |
| C_1 | Coefficients of Biot number for cylinders |
| D_i | Inner diameter of the detonation tube (m) |
| D_o | Outer diameter of the detonation tube (m) |
| D_1 | Inner diameter of the water jacket (m) |
| D_2 | Outer diameter of the water jacket (m) |
| h_c | Overall heat transfer coefficient $\left(\frac{W}{m^2.K}\right)$ |
| J_0 | Bessel Function |
| \dot{m} | Mass flow rate of water inside the tube $\left(\frac{kg}{s}\right)$ |
| \dot{m}_i | Mass flow rate at the inlet $\left(\frac{kg}{s}\right)$ |

| | |
|------------------|--|
| \dot{m}_e | Mass flow rate at the exit section $\left(\frac{kg}{s}\right)$ |
| \bar{P} | Average pressure of the burned gas (<i>atm</i>) |
| P_i | Pressure at the inlet (<i>atm</i>) |
| Q | Heat dissipated by the PDE (<i>kJ</i>) |
| \bar{T} | Average exit temperature of the gas (<i>K</i>) |
| T_{ej} | CJ detonation temperature (<i>K</i>) |
| T_3 | Taylor rarefaction wave temperature (<i>K</i>) |
| $T_{reflection}$ | Average gas temperature during reflection (<i>K</i>) |
| $T_{Blow\ down}$ | Average gas temperature during blow down (<i>K</i>) |
| T_i | Inlet temperature of the fuel and oxidizer mixture (<i>K</i>) |
| t_{det} | Time taken for detonation process (<i>s</i>) |
| t_{fill} | Time taken for filling process (<i>s</i>) |
| t_{purge} | Time taken for purging process (<i>s</i>) |
| t_{rar} | Time taken for rarefaction process (<i>s</i>) |
| T_{w1}, T_{w2} | Temperatures of the inner and outer walls of the detonation tube (<i>K</i>) |

| | |
|-----------------|---|
| T_∞ | Ambient temperature (300 Kelvin) |
| ν | Kinematic viscosity |
| v_i | Inlet velocity of the fuel oxide mixture $\left(\frac{m}{s}\right)$ |
| v_e | Exit velocity of the burned gas $\left(\frac{m}{s}\right)$ |
| V_i, V_e | Inlet and exit volumes of the detonation tube (m^3) |
| v_{fill} | Velocity at which the detonation tube is filled with fuel |
| v_{purge} | Velocity at which air is blown into the detonation tube $\left(\frac{m}{s}\right)$ |
| x | Reference location inside the detonation tube (m) |
| x_L | Length of the detonation tube (m) |
| x_L | Length of the detonation tube (m) |
| $\rho_{e(avg)}$ | Average exit density of the burned gas $\left(\frac{kg}{m^3}\right)$ |
| ρ_i | Inlet density of fuel and oxide mixture H_2 and O_2 $\left(\frac{kg}{m^3}\right)$ |
| γ | Ratio of specific heats. |
| θ^* | Non-dimensional parameter |

Subscripts

| | |
|-----|---|
| i | Inlet section of the PDE |
| e | Exit section of the PDE |
| 1 | Initial conditions inside the detonation tube |
| 2 | Final conditions inside the detonation tube |

CHAPTER 1

INTRODUCTION

1.1 Pulse Detonation Engine

The pulse detonation engines are a type of engines which are simple in construction, lighter in weight, have negligible moving parts and produce large amounts of thrust. Much research has been carried out on these propulsion systems for many years due to the numerous advantages these engines have over traditional jet engines. Compared with turbojets and turbofans, these engines are simple in geometry with a long tube, technically termed the detonation tube, which is open at one end and closed at the other end. The closed end of the tube has valves to control the flow of fuel and oxidizer mixture (Hydrogen and Oxygen in this case) into the tube. These engines minimize the use of compressors to compress the air before combustion, thereby reducing the overall weight and complexity of the engine. However at low flight velocities a compressor is required to pump air into the chamber. The basic block diagrams of the turbojet engine and the PDE are shown in the following figures.

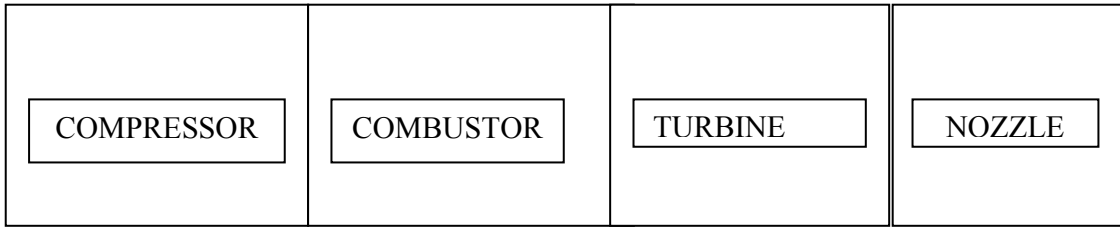


Fig 1.1 Block Diagram of a Turbojet Engine

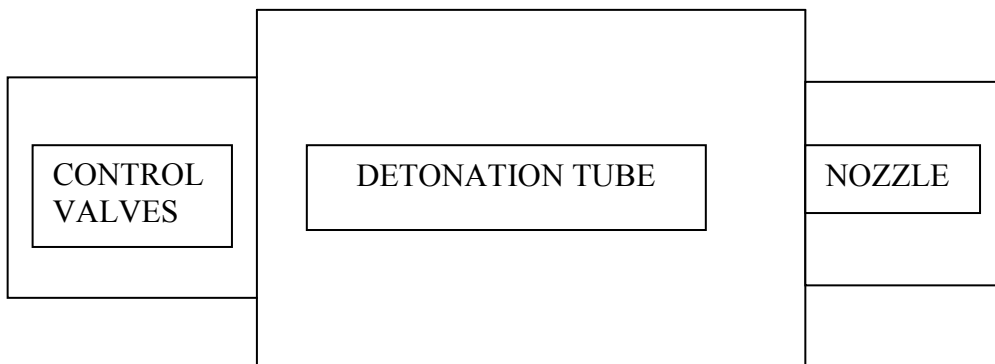


Fig 1.2 Block Diagram of a Pulse Detonation Engine

The detonation process, in addition to producing huge amounts of thrust, also aids in producing high temperatures and pressures and hence this engine has high efficiencies when compared with other engines. The following figure outlines the various processes that are part of the pulse detonation cycle.

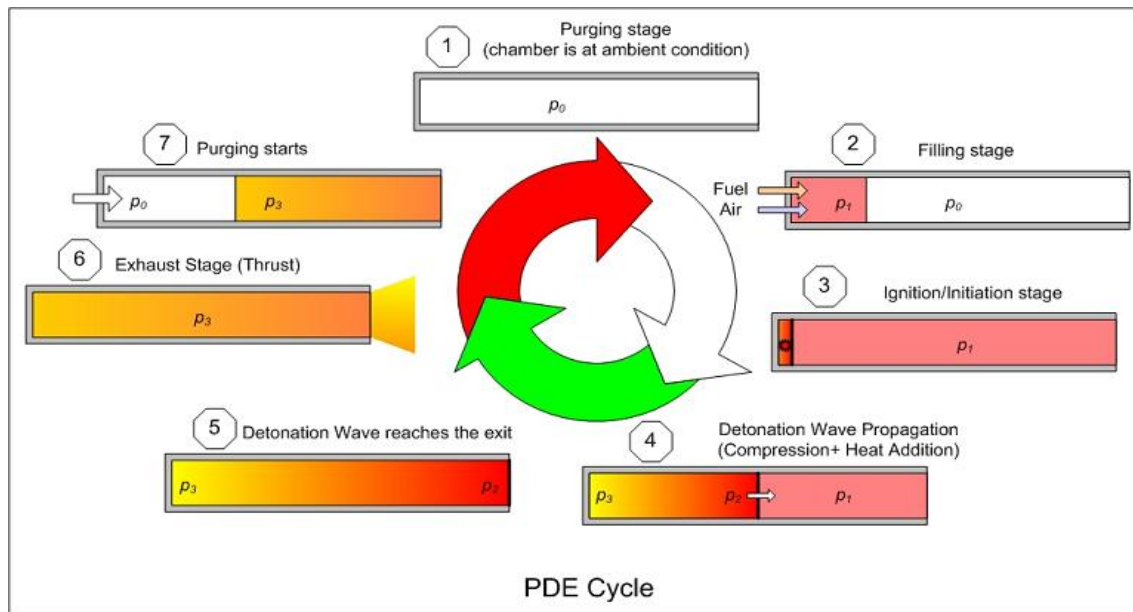


Fig 1.3 Schematic of a Pulse Detonation Cycle

The various processes that are illustrated in the above figure (fig 1.3) are explained in detail in the following sections. The Gas dynamic analysis of the PDE cycle follows the model developed by Takuma Endo and Toshi Fujiwara (Ref. 1).

1.1.1 Filling Process

This is the 1st process that takes place in the pulse detonation cycle. This process is simply filling the detonation tube with stoichiometric mixture of fuel and oxidizer at a certain design velocity. The time taken for this process should be minimized, because a slight delay in filling would have an impact on the timing of the remaining process and ultimately lead to a delayed detonation. The cross section of a detonation tube is shown below and the filling time is calculated as follows,

Fig 1.4 Cross Section of a Detonation Tube

If x_L is the length of the detonation tube, then the filling time is calculated as,

$$t_{fill} = \frac{\text{length of the tube}}{\text{filling Velocity}} = \frac{x_L}{v_{fill}}$$

The quantity v_{fill} is the velocity with which the mixture of the fuel and oxidizer mixture is pumped into the detonation tube. The value of v_{fill} is assumed to be some practically feasible value i.e. 20m/s, 30m/s.....100m/s....The higher the flow velocity, the lesser the filling time and ultimately lesser cycle times. The value of filling velocity should be carefully assumed as for achieving higher flow rates, a highly efficient pumping system should be incorporated.

1.1.2 CJ Detonation Process

This is the process taking place after the filling process. The moving mixture is detonated at the closed end of the detonation tube, which creates a wave which moves at very high velocities towards the open end. Compared with the filling process, this process takes place at a fraction of a millisecond as high temperatures gases travel along the tube with velocities typically a few thousand meters per second. The velocity with

which the detonation wave travels from the open end to the closed end is termed the detonation velocity. The Detonation time of this wave is calculated as

$$t_{1/2} = \frac{\text{length of the tube}}{\text{CJ wave Velocity}} = \frac{x_L}{D_{cj}} \quad [\text{Fig 1.4}]$$

The value of D_{cj} is obtained from the NASA Chemical Equilibrium Applications code

(adapted from Ref .2) for a fuel and oxidizer mixture when detonated.

1.1.3 Taylor Rarefaction Process

This is the process which is assumed to be taking place simultaneously with the detonation wave. As the detonation wave moves towards the open end of the tube, the fuel and the oxidizer valves are closed and since the gas attached to the closed end should be at rest, the flow of gas between the CJ detonation wave and the closed end is decelerated. This deceleration results in the generation of a rarefaction wave which follows the detonation wave. Since the front boundary of the Taylor wave coincides with that of the CJ wave, the front boundary conditions of this wave are similar to the CJ conditions of the flow (adapted from Ref. 1). The time taken by the trailing edge of the rarefaction wave to reach the end of the detonation tube is (Ref. 1).

$$t_1 = \frac{\text{length of the tube}}{\left(\frac{\text{Detonation velocity}}{2}\right)} = \frac{x_L}{\left(\frac{D_{cj}}{2}\right)}$$

1.1.4 Reflected Rarefaction and Exhaust Process

At time $t = t_1$, the Taylor wave exits the detonation tube. During this process, another rarefaction wave is generated which starts to propagate back towards the closed end. The front boundary condition travels at sonic velocity and reaches the closed end at $t = t_{II}$. The reflected rarefaction wave is an expansion wave which drops the pressure inside the tube, but the pressure is still above ambient thus the flow continues to evacuate the tube. This phase is called exhaust phase and lasts for certain time period t_{III} (adapted from Ref. 1). During this process, the burned gas is exhausted from the open end of the tube. Also during the time period t_{II} to t_{III} , the pressure is assumed to decay linearly with time until it reaches ambient conditions. However, the final temperature of this process is still very high. The time for rarefaction process is calculated as follows (Ref. 1).

$$t_{II} = \frac{\text{length of the tube}}{\text{rarefaction velocity}} = \frac{x_L}{\left(\frac{D_{cj}}{4}\right)}$$

Fig 1.5 Sectional View of the Detonation Tube

$$t_{III} = \left[1 + \left(\frac{\gamma_2 + 1}{2} \right)^{\frac{\gamma_2 + 1}{\gamma_2 - 1}} \right] \frac{x_L}{\left(\frac{D_{cj}}{2}\right)}$$

The time taken by the rarefaction wave in traveling through the detonation tube will be much higher than that of the detonation wave as the velocities of the rarefaction wave are much lower than the detonation wave.

1.1.5 Purging Process

This is the final process in the pulse detonation cycle. This takes place after the rarefaction process as shown in fig 1.4. This process involves pumping air at high velocities into the detonation tube, in order to clean the tube of any burnt impurities left inside the tube after the detonation and rarefaction process. This process is very vital as in the absence of this process, high temperature particles inside the detonation tube can cause the fuel-air mixture to auto ignite and ultimately lead to deflagration. This process can be referred to as scavenging the detonation tube before the filling process. The time taken for this process is calculated on the same lines as of the filling process, the only difference being, in the later, fuel and oxidizer mixture is pumped into the detonation tube, where as in the former, only air is pumped to force the burnt particles out of the tube. Thus, purging time is given by

$$t_{purge} = \frac{\text{length of the tube}}{\text{purging Velocity}} = \frac{x_L}{v_{purge}}$$

The value of v_{purge} in the above expression, plays a vital role as the purging time is inversely proportional to the purging velocity. It is generally presumed that the value of

v_{purge} is assumed to be some practically feasible value i.e. 20m/s, 30m/s.....100m/s....The higher the purge velocity, the lower the purge time and ultimately faster cycle times can be achieved .

1.2 Objective Of Current Research

Inspite of possessing many advantages, for example; faster cycle times, negligible moving parts, high thrust production, the vital factor affecting the practical implementation of PDEs is the high temperatures that are produced during the normal mode of operation. The temperatures produced during one cycle of operation, may be very high (on the order of 3000K). Thus in order to ensure that these engines operate for a longer duration, proper and efficient cooling system designs should be incorporated. The current research aims to conduct a thermal analysis of the engine and proposing a preliminary heat exchanger design.

1.3 Chemical Equilibrium Applications

Chemical Equilibrium Applications (Ref .2) is computer program which calculates the chemical equilibrium product concentrations and thermodynamic properties for any set of reactants at a given temperature and pressure. The input to the code is an equilibrium mixture of fuel and oxidizer which are taken to be Hydrogen and Oxygen at 300 Kelvin in the current analysis. The code then calculates the thermodynamic properties after a

Chapman Jouguet Detonation, which is one type of detonation. The code also calculates all the thermodynamic properties of the detonated mixture.

1.4 Energy Analysis of Unsteady-Flow Processes

The process during which there is a rapid change in the fluid properties over a certain time period is generally termed an unsteady flow process. While analyzing these kinds of processes, it is important to keep track of the mass and energy contents of the control volume as well as the energy flux across the boundary.

The mass balance for any system undergoing any process can be expressed as

$$m_i - m_{out} = \Delta m_{system}$$

Where $\Delta m_{system} = m_{final} - m_{initial}$ is the change in the mass of the system. For control volumes, it can be expressed as

$$m_i - m_e = (m_2 - m_1)_{CV}$$

Where i = inlet, e = exit, 1 = initial state, 2 = final state. Often unsteady flow processes can be modeled as a uniform state, uniform flow process, which requires that the fluid properties within the control volume vary only with time. The energy balance relations for a uniform flow system are expressed as (adapted from Ref. 3).

$$Q - W = (mh_t)_e - (mh_t)_i + (m_2 u_{t2} - m_1 u_{t1}) \quad (1.4.1)$$

Since there is no shaft work imparted to the system, neglecting W in the above equation (1.4.1), the final energy expression for an unsteady flow process is expressed as

$$Q = (mh_t)_e - (mh_t)_i + (m_2u_{t2} - m_1u_{t1}) \quad (1.4.2)$$

Where

$$h_{te} = C_p T_e + \frac{v_e^2}{2} \quad (1.4.3)$$

$$h_{ti} = C_p T_i + \frac{v_i^2}{2} \quad (1.4.4)$$

$$u_{t1} = C_v T_1 + \frac{v_1^2}{2} \quad (1.4.5)$$

$$u_{t2} = C_v T_2 + \frac{v_2^2}{2} \quad (1.4.6)$$

CHAPTER 2

DETERMINATION OF THERMODYNAMIC PROPERTIES USING CHEMICAL EQUILIBRIUM APPLICATIONS CODE

2.1 Input to the CEA Code

The input to the Chemical Equilibrium Applications code is the temperature and pressure of a mixture of hydrogen and oxygen.

Inlet Temperature: 300 K

Inlet Pressure: 1 atm

The following images outline a sample CEA application using a mixture of fuel/oxidizer. The type of thermodynamic reaction desired is the Chapman Jouquet detonation as shown highlighted in the following figure.

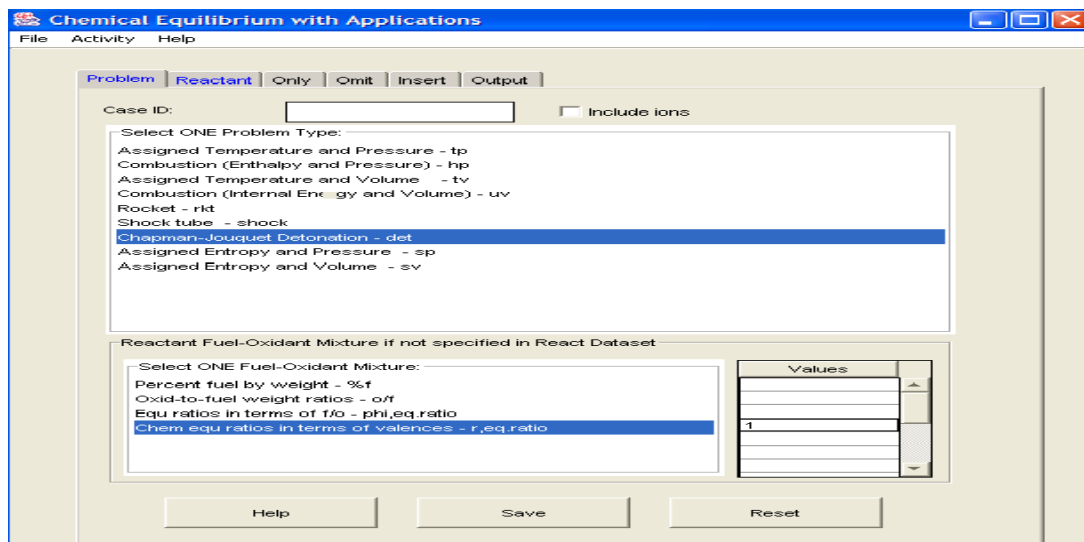


Fig 2.1 Input Section of the CEA Code for Hydrogen and Oxygen

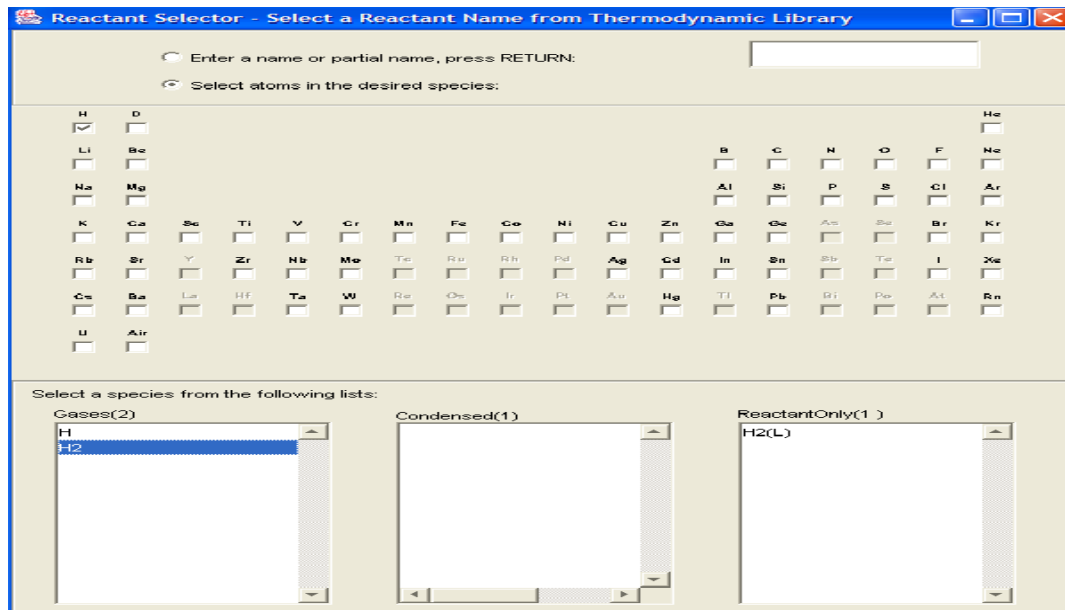


Fig 2.2 Fuel Selection Section of the CEA Code

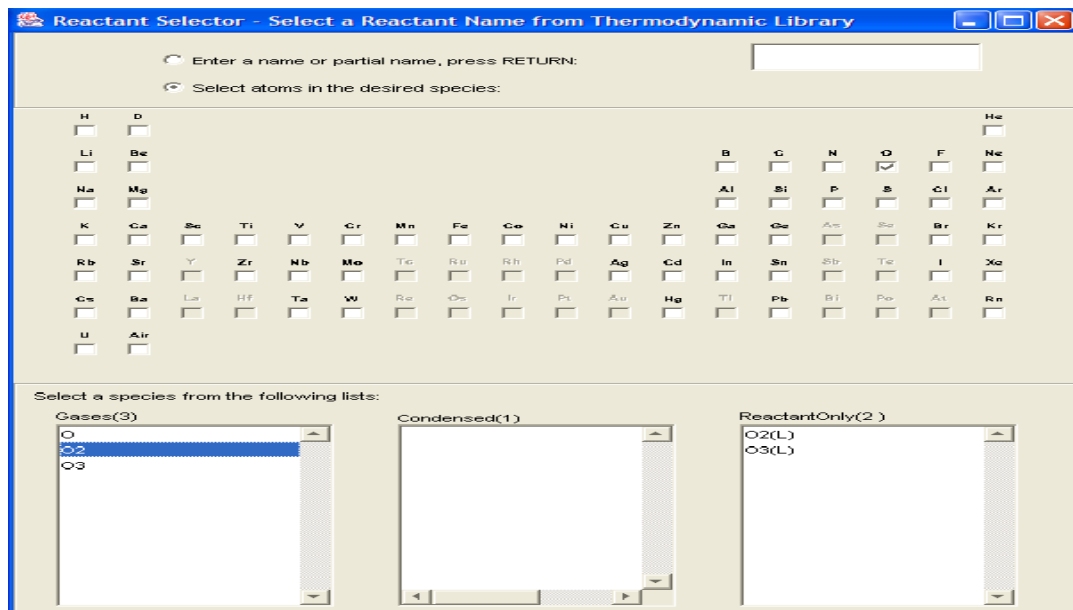


Fig 2.3 Oxidizer Selection Section of the Code

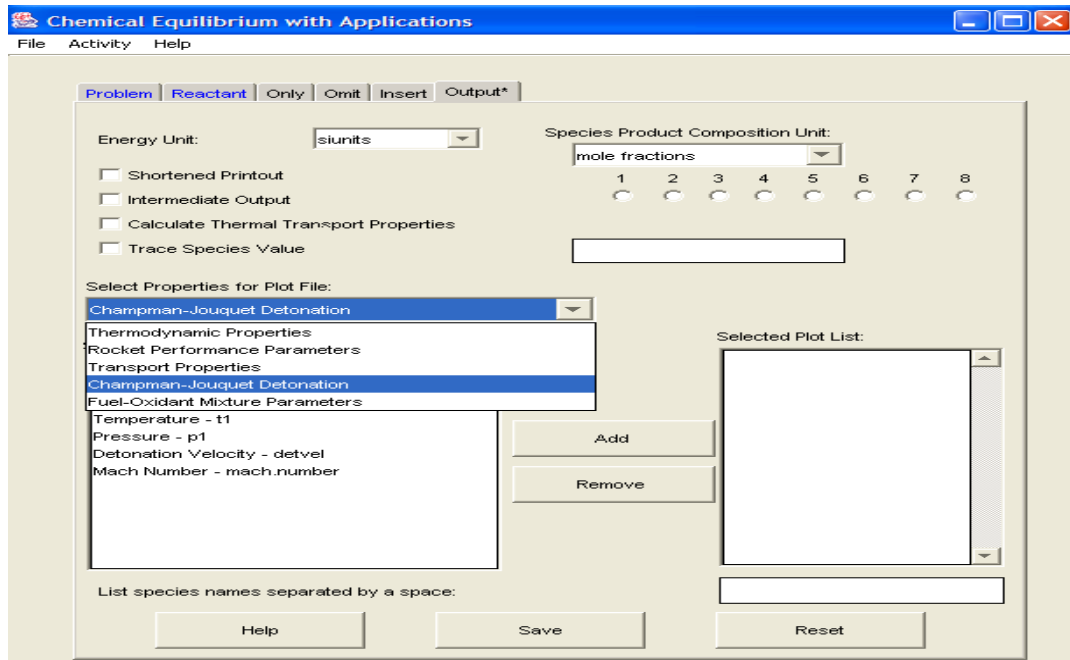


Fig 2.4 Type of Detonation Selection Section of the CEA Code

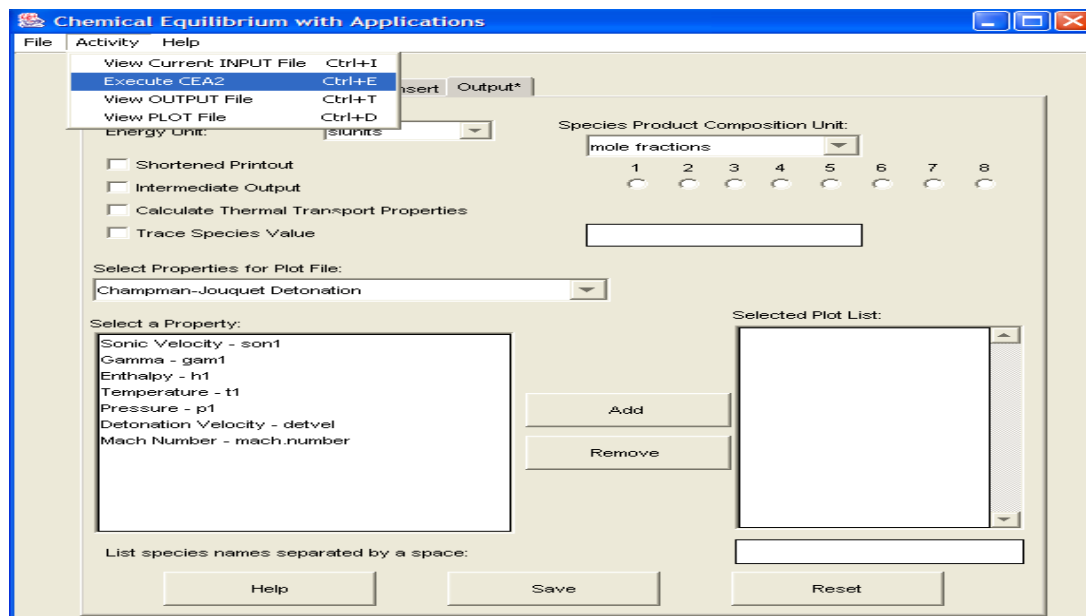


Fig 2.5 Execution Section of the CEA CODE

2.2 Output from the CEA Code

After entering the input values to the code, the code calculates the Chapman Jouguet detonation properties of the mixture. The exit values are generally denoted with a subscript CJ (adapted from Ref.2) representing the values obtained at Chapman Jouguet detonation. The values of thermodynamic properties after the Chapman Jouguet detonation are tabulated below.

Table 2.1 Thermodynamic Properties After CJ Detonation Process (CEA)

| | | | |
|-----------------------|-----------------------|----------|------------------------|
| D_{cj} | P_{cj} | T_{cj} | ρ_{cj} |
| 2835 m/s | 18.6 atm | 3675 K | 0.89 kg/m ³ |
| $\gamma_1 = \gamma_p$ | $\gamma_2 = \gamma_c$ | M_{cj} | R |
| 1.4014 | 1.1288 | 5.2562 | 573.41 J/(kg.K) |

CHAPTER 3

AVERAGE THERMODYNAMIC PROPERTIES FOR ONE CYCLE

3.1 Filling Process

Initially, the tube is completely filled with a uniform detonable mixture of hydrogen and oxygen, the properties of which are characterized by $p_1 = 1 \text{ atm}$, $T_1 = 300\text{K}$ and $u_1 = 0$ as the mixture is at rest. The time taken by this process is expressed as

$$t_{fill} = \frac{x_L}{v_{fill}} = \frac{1(m)}{50 m/s} = 0.02 s .$$

After this time period, the detonation tube is assumed to be

completely filled with the fuel and oxidizer mixture. The initial and final conditions of the flow during this process are equal as there are no thermodynamic interactions taking place.

3.2 CJ Detonation Process

After the tube is completely filled with the fuel and oxidizer mixture, a shock wave is generated at the closed end of the tube which travels with high velocity towards the open end of the tube. This shock wave compresses the fuel mixture thereby resulting in enormous increase in the values of the thermodynamic properties ahead of it. The time taken by this wave to reach the open end of the tube is termed as the detonation time.

This time as explained in the first chapter, is expressed as $t_{1/2} = \frac{x_L}{D_{ej}}$, where $x_L = 1\text{m}$

and $D_{cj} = 2835$ m/s (CJ wave velocity), hence $t_{1/2} = \frac{1(\text{m})}{2835\left(\frac{\text{m}}{\text{s}}\right)} = 0.00035$ s. The NASA

CEA code (adapted from Ref.2) is utilized to calculate the properties of the combustion products after CJ detonation. The CJ detonation properties of the mixture are obtained from Table 2.1 as

$$T_{cj} = 3675 \text{ K}$$

$$p_{cj} = 18.6 \text{ atm}$$

$$\rho_{cj} = 0.89 \frac{\text{kg}}{\text{m}^3}$$

The following analysis is based on the Endo-Fujiwara model of analyzing the PDE (Ref.1) .The above obtained values from the CEA code are compared with the following Hugoniot relations for the CJ conditions derived from the Endo-Fujiwara model.

$$\rho_2 = \frac{\gamma_2 + 1}{\gamma_2} \rho_1 = 0.86 \frac{\text{kg}}{\text{m}^3} \quad (3.2.1)$$

$$p_2 = \frac{\gamma_1}{\gamma_2 + 1} M_{CJ}^2 p_1 = 18.12 \text{ atm} \quad (3.2.2)$$

$$T_2 = \frac{p_2}{\rho_2 R} = 3662.46 \text{ K} \quad (3.2.3)$$

The values of the thermodynamic properties calculated by the CEA code are approximately equal to the analytically calculated values from the above expressions

The Hugoniot relations are used as a basis to compare with the results from the CEA code and also to calculate the conditions of the flow during the other processes.

3.3 Taylor Rarefaction Wave Process

As the detonation wave travels from the closed end to the open end of the tube, it is followed by Taylor rarefaction waves, caused by the end wall boundary conditions. This process lasts for a certain time period $t_{1/2} \leq t \leq t_1$, where $t_{1/2} = 0.35$ ms and $t_1 = 0.71$ ms. The leading edge of the Taylor rarefaction wave follows immediately behind the detonation wave and hence the front boundary conditions of these waves are equal to that of the CJ values.

3.3.1 Front Boundary Conditions of Taylor Rarefaction Wave

$$T_2 = 3662.46 \text{ K (From equation 3.2.3)}$$

$$p_2 = 18.12 \text{ atm (From equation 3.2.2)}$$

$$\rho_2 = 0.86 \frac{\text{kg}}{\text{m}^3} \text{ (From equation 3.2.1)}$$

The state of the flow inside the rarefaction wave is written by the relations for the self similar rarefaction waves as (adapted from Ref. 1)

$$p = \left[\left(\frac{1}{\gamma_2} + \frac{\gamma_2 - 1}{\gamma_2} \left(\frac{x}{x_2} \right) \right)^{\frac{2\gamma_2}{\gamma_2 - 1}} p_2 \right] \quad (3.3.1)$$

$$\rho = \left[\left(\frac{1}{\gamma_2} + \frac{\gamma_2 - 1}{\gamma_2} \left(\frac{x}{x_2} \right) \right)^{\frac{2}{\gamma_2 - 1}} \rho_2 \right] \quad (3.3.2)$$

$$u = u_2 - \frac{2(x_2 - x)}{(\gamma_2 + 1)t} \quad (3.3.3)$$

The temperature is calculated from the equation of state as

$$T = \frac{p_2}{\rho_2 R} \quad (3.3.4)$$

where $R = 573 \frac{J}{kg.K}$ from table 2.1 and p_2, ρ_2 are obtained from 3.3.1. In the above expressions, x_2 is the position of the CJ surface expressed as $x_2 = D_{c_j}t$ and x is the variable length from the trailing edge to the leading edge of the Taylor wave. The trailing edge of the Taylor wave is assumed to be $\frac{x_2}{2}$, thus when the leading edge of the wave reaches the end of the tube ($x_2 = x_L$), the trailing edge is at $x_2 = \frac{1}{2}x_L$. All the required variables are substituted in the above expressions and the properties of the burned mixture during the Taylor rarefaction wave are calculated at different locations inside the detonation chamber. The velocity at the trailing edge of the Taylor wave is zero, and the thermodynamic properties are constant from the trailing edge of the wave to the end wall, and are given by the end wall values of T_3, p_3, ρ_3 which are expressed by the following relations.

$$p_3 = \frac{\gamma_1}{2\gamma_2} \left(\frac{\gamma_2 + 1}{2\gamma_2} \right)^{\frac{\gamma_2 + 1}{\gamma_2 - 1}} M_{cj}^2 p_1 \quad (3.3.5)$$

$$\rho_3 = 2 \left(\frac{\gamma_2 + 1}{2\gamma_2} \right)^{\frac{\gamma_2 + 1}{\gamma_2 - 1}} \rho_1 \quad (3.3.6)$$

$$T_3 = \frac{p_3}{\rho_3 R} \quad (3.3.7)$$

3.3.2 End Wall Conditions of Taylor Rarefaction Wave

$$T_3 = 3256.48 \text{ K}$$

$$p_3 = 6.47 \text{ atm}$$

$$\rho_3 = 0.34 \frac{\text{kg}}{\text{m}^3}$$

The above expressions (3.3.1 to 3.3.4) are solved using Mathematica and the values are obtained for this process over the length of the detonation tube.

All the obtained values are plotted at the time $t = t_{1/2}$. The variation in the conditions of the flow during this process is shown in Fig 3.1 to 3.3

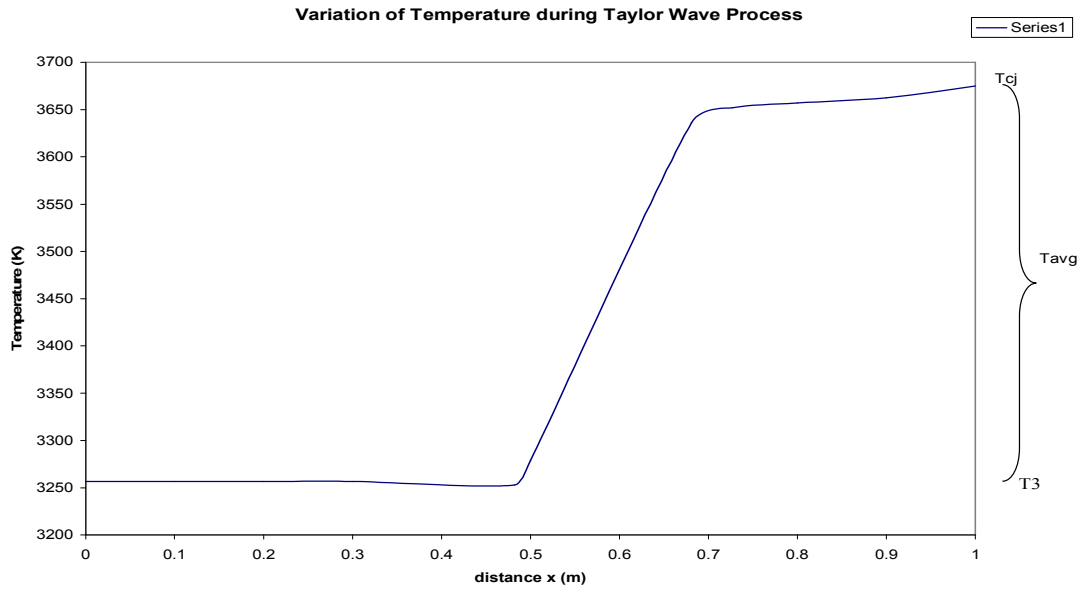


Fig 3.1 Variation of Temperature During Taylor Wave Process

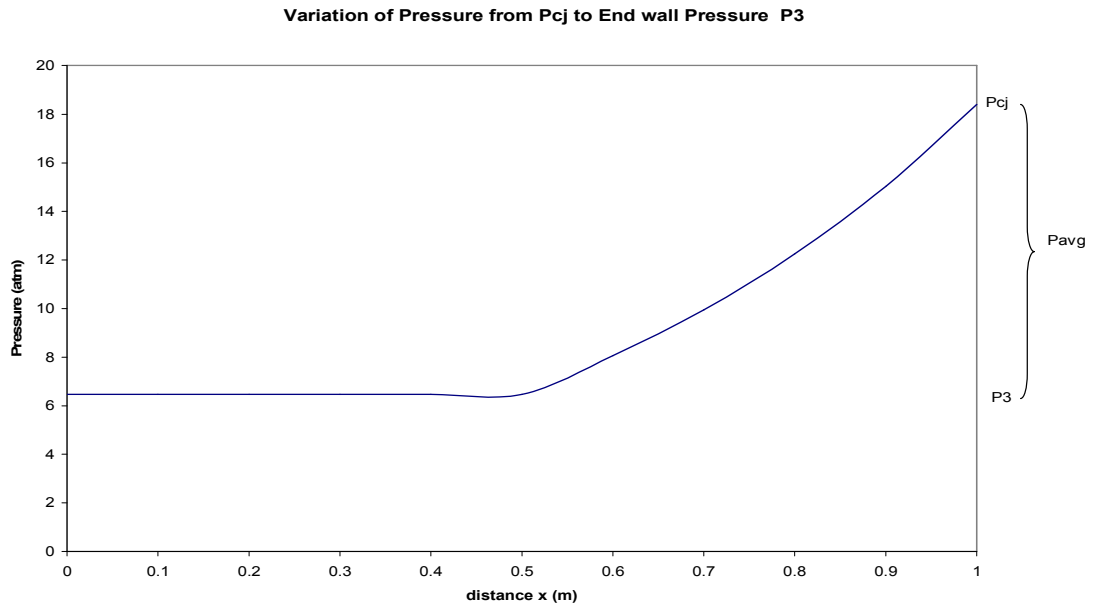


Fig 3.2 Variation of Pressure During Taylor Wave Process

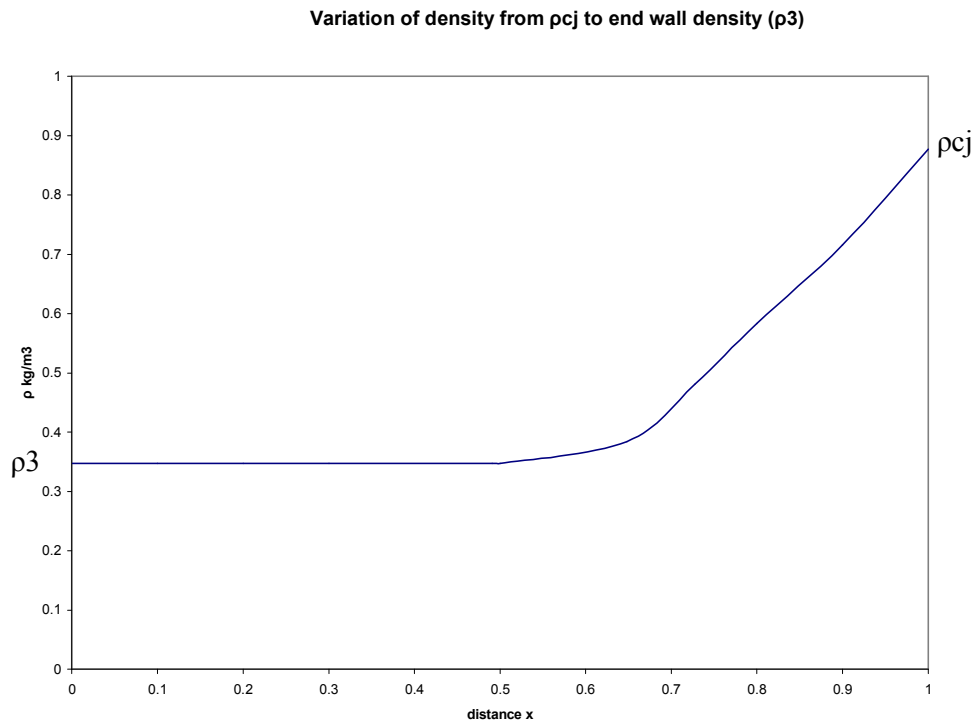


Fig 3.3 Variation of Density During Taylor Wave Process

3.3.3 Average Conditions of Flow During Detonation Process

$$\bar{T} = 3297 K$$

$$\bar{p} = 7.9 atm$$

$$\bar{\rho} = 0.40 \frac{kg}{m^3}$$

Also at time $t_l = 0.71 ms$, the Taylor wave exits the detonation tube and hence the conditions of the gas during this period will be constant throughout the tube and will be equal to the end wall conditions T_3, p_3, ρ_3 . The plots for the above case are shown below for reference.

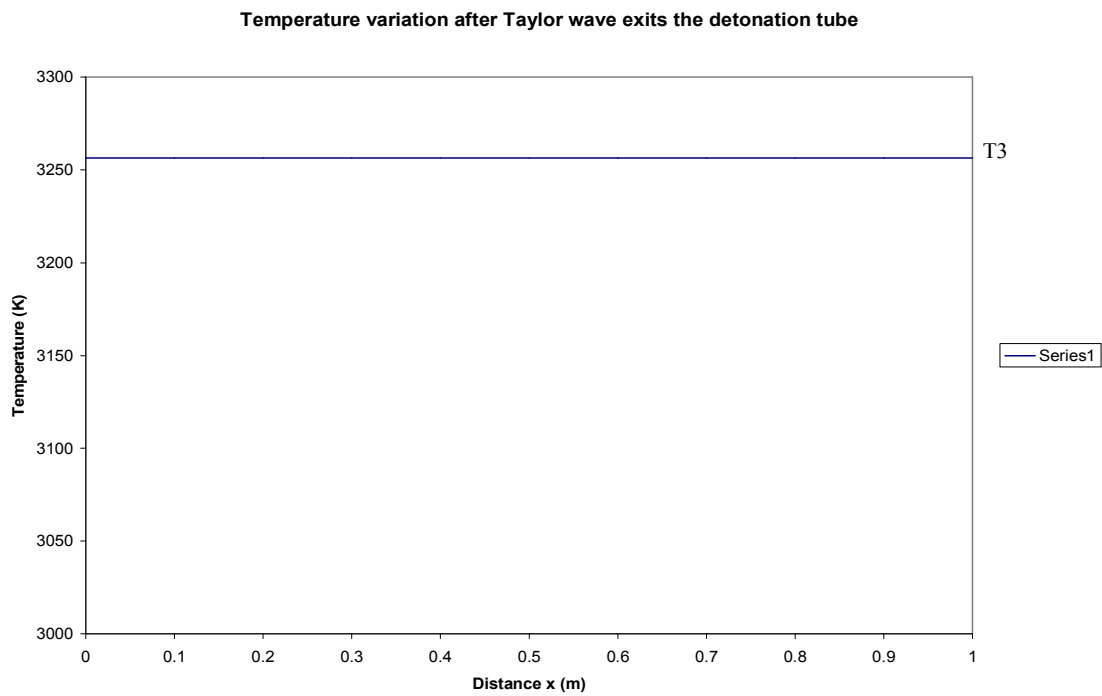


Fig 3.4 Temperature Variation After Taylor Wave Process

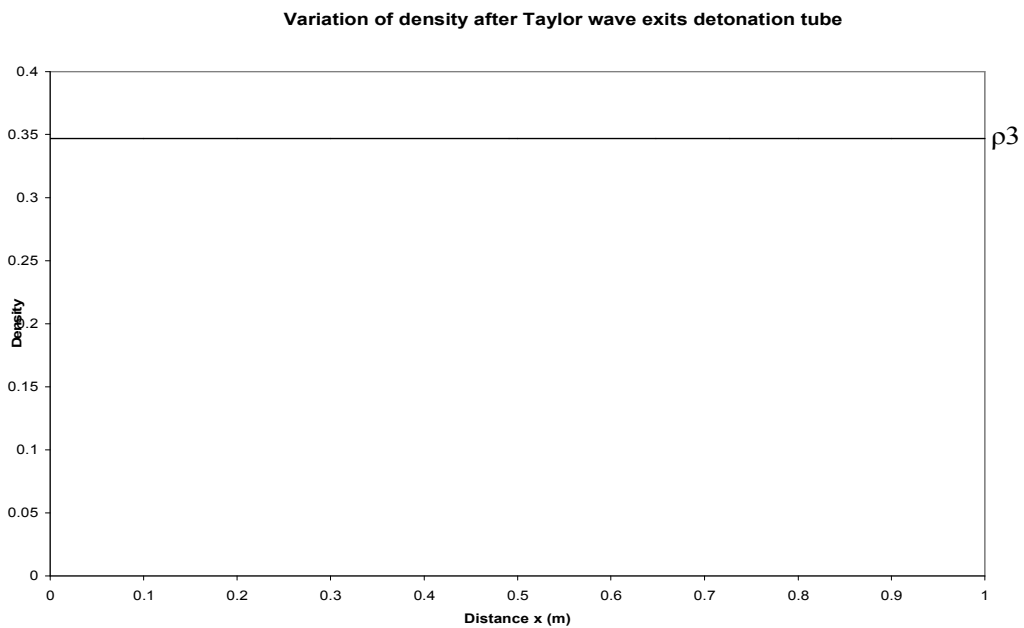


Fig 3.5 Density Variation After Taylor Wave Process

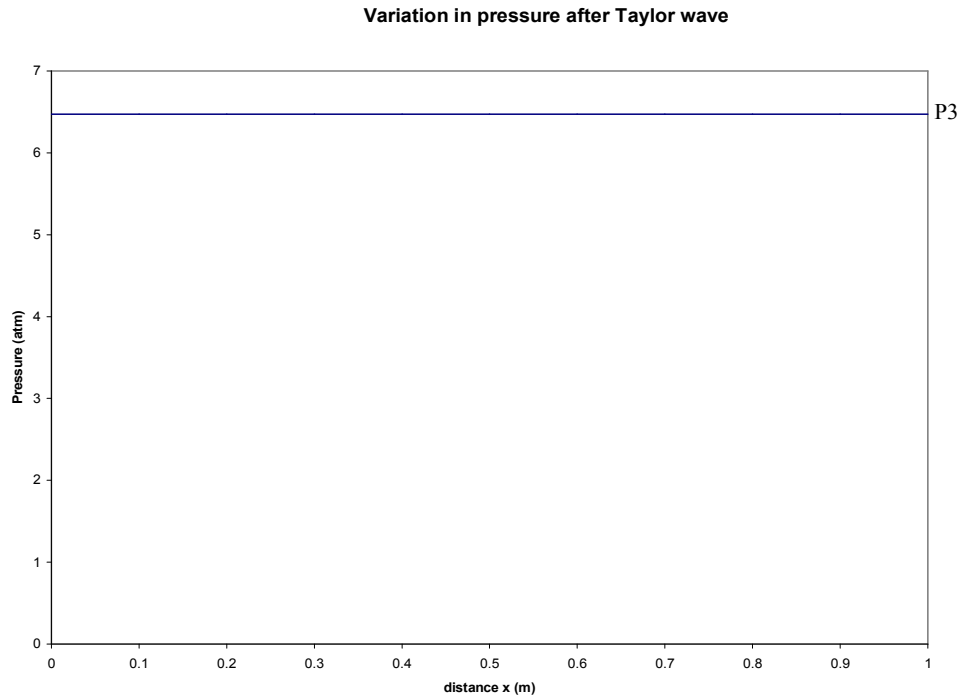


Fig 3.6 Pressure Variation After Taylor Wave Process

3.4 Reflected Rarefaction Process

As the detonation wave along with the Taylor rarefaction waves reach the open end of the tube, a reflected wave is generated that travels from the open end back towards the closed end. The value of T_3, p_3, ρ_3 which are the end wall conditions after the Taylor rarefaction process, are the initial conditions for this process.

3.4.1 Initial Conditions of Reflection Process

$$T_3 = 3256.48 K ,$$

$$p_3 = 6.47 atm ,$$

$$\rho_3 = 0.34 \frac{kg}{m^3}.$$

The conditions of the flow during the reflection process are given by the following expressions for a self similar rarefaction wave.

$$p = \left[\left(1 + \frac{\gamma_2 - 1}{D_{cj}} \frac{x_L - x}{t - t_1} \right)^{\frac{2\gamma_2}{\gamma_2 - 1}} \right] p_{ex} \quad (3.4.1)$$

$$\rho = \left[\left(1 + \frac{\gamma_2 - 1}{D_{cj}} \frac{x_L - x}{t - t_1} \right)^{\frac{2}{\gamma_2 - 1}} \right] \rho_{ex} \quad (3.4.2)$$

$$T = \frac{p}{\rho R} \quad (3.4.3)$$

The exit conditions of gas after the rarefaction wave are written by the relation for the self similar rarefaction waves as follows.

$$p_{ex} = \left[\frac{\gamma_1}{\frac{2\gamma_2}{\gamma_2^{\gamma_2 - 1}(\gamma_2 + 1)}} M_{cj}^2 P_i \right] \quad (3.4.4)$$

$$\rho_{ex} = \left[\frac{\frac{\gamma_2 - 1}{\gamma_2 + 1}}{\gamma_2^{\frac{\gamma_2 - 1}{2}}} \right] \rho_1 \quad (3.4.5)$$

$$T_{ex} = \frac{p_{ex}}{\rho_{ex} R} \quad (3.4.6)$$

3.4.2 Final Conditions of Reflection Process

$$T_{ex} = 2874.35 K$$

$$p_{ex} = 2.16 atm$$

$$\rho_{ex} = 0.13 \frac{kg}{m^3}$$

Similar to 3.3, the average values during this process are obtained using Mathematica. The initial conditions are obtained from 3.4.1 and the final conditions are obtained from section 3.4.2. The following profiles are obtained for all the above expressions and the variation in conditions of the flow during the reflection process is shown below for reference.

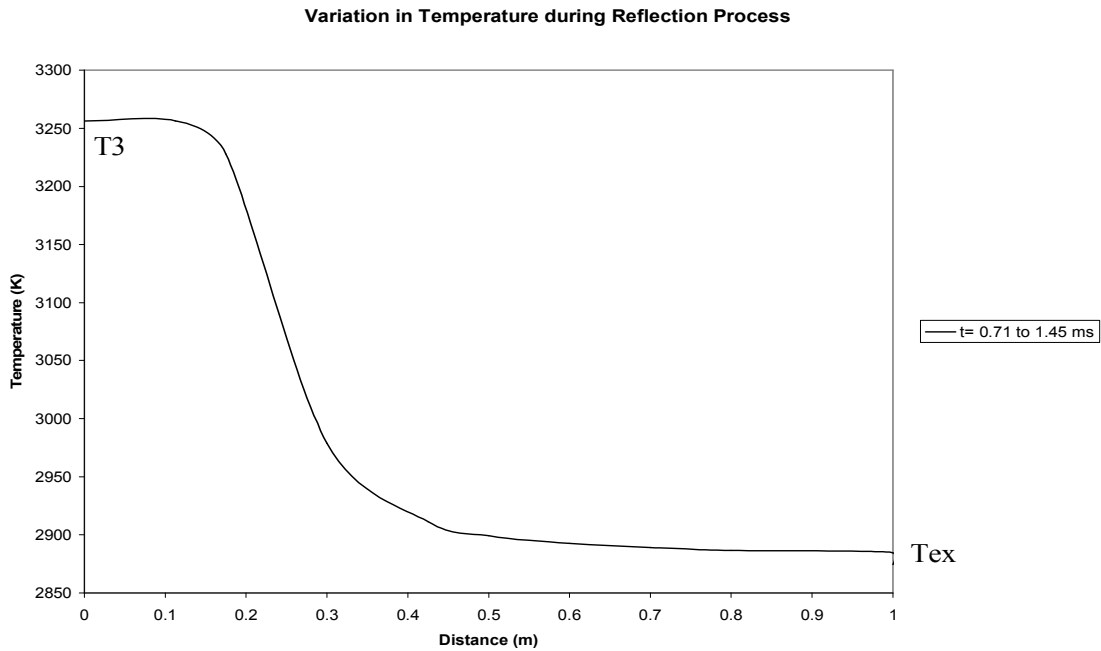


Fig 3.7 Variation in Temperature During Reflection Process

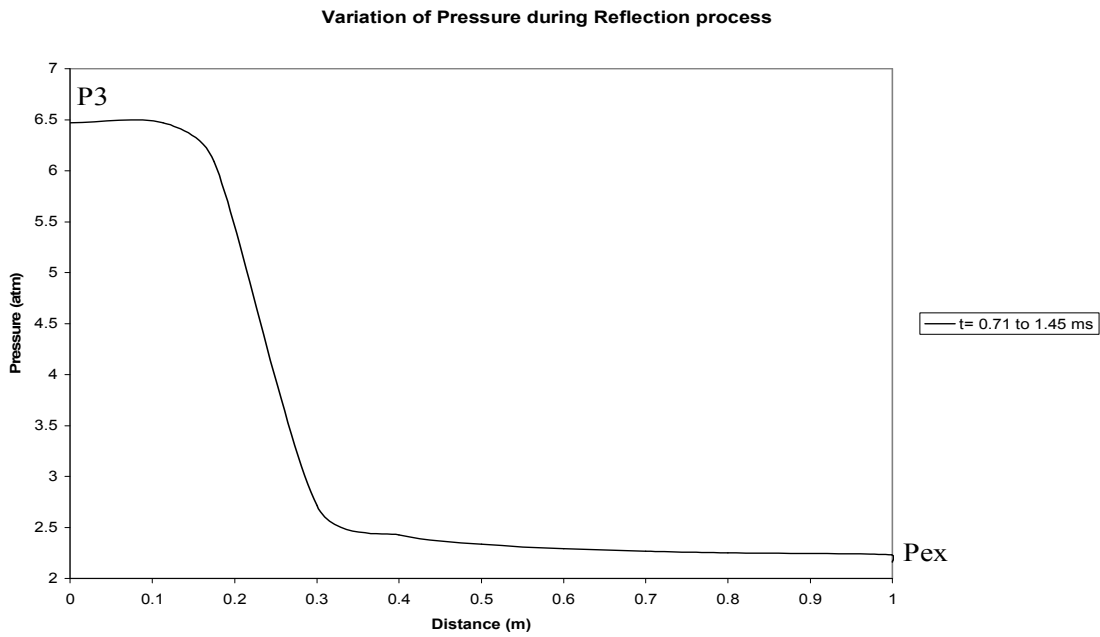


Fig 3.8 Variation in Pressure During Reflection Process

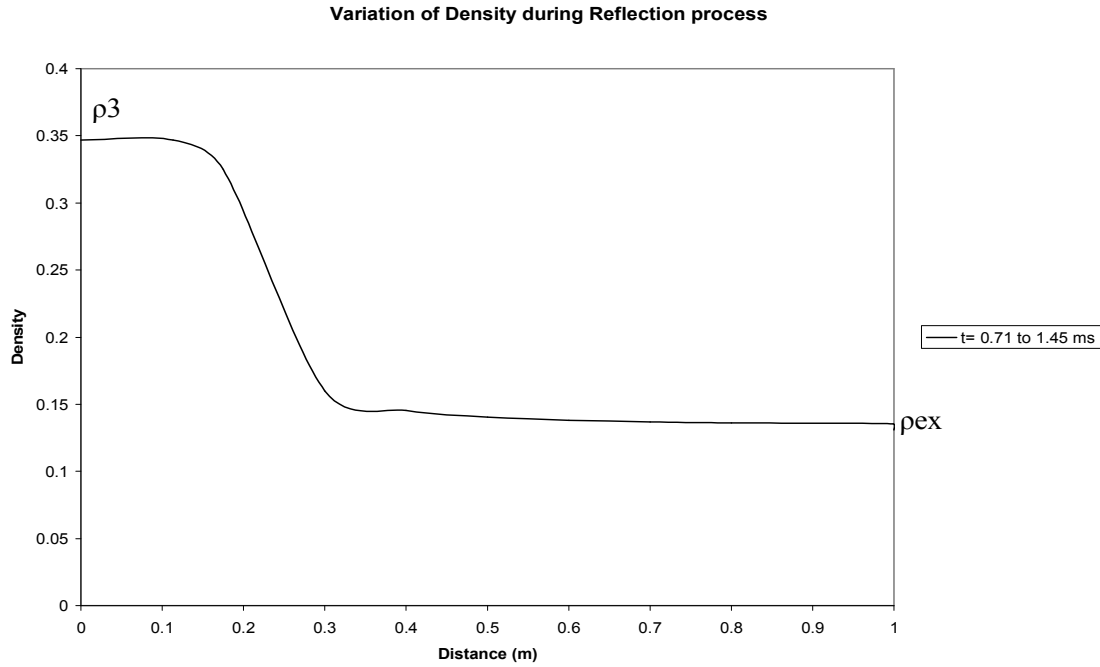


Fig 3.9 Variation in Density During Reflection Process

3.4.3 Average Conditions of Flow During Reflection Process

$$\bar{T} = 3045.08 K$$

$$\bar{p} = 4.04 atm$$

$$\bar{\rho} = 0.22 \frac{kg}{m^3}$$

3.5 Blow Down Process

The reflected rarefaction wave after colliding with the closed end of the tube gets reflected to the open end once again and hence in this process another rarefaction wave is generated and starts to propagate through the tube from the closed end to the open end. The time taken by the rarefaction wave will be much higher than the time taken by the detonation wave which is evident in the velocity values of the two waves. The time

is thus given as
$$t_{III} = \left[1 + \left(\frac{\gamma_2 + 1}{2} \right)^{\frac{\gamma_2 + 1}{\gamma_2 - 1}} \right] \frac{2x_L}{D_{cj}} = 2.6 \text{ ms.}$$

3.5.1 Initial Conditions of Blow Down Process

$$T_3 = 3256.48 K ,$$

$$p_3 = 6.47 atm \ \&$$

$$\rho_3 = 0.34 \frac{kg}{m^3} .$$

During the blow down process, the gas is assumed to be isentropic and hence isentropic relations are used to determine the end conditions of the flow. During this process, the pressure is assumed to decay linearly from an initial value of p_3 to ambient conditions.

The temperature and density decay are calculated from isentropic relations. All the

obtained values are then averaged for the entire process. Hence the end conditions of this process are given by the isentropic relations expressed as

$$\left(\frac{p_2}{p_1}\right) = \left(\frac{\rho_2}{\rho_1}\right)^\gamma = \left(\frac{T_2}{T_1}\right)^{\frac{\gamma}{\gamma-1}} \quad (3.5.1)$$

$$p(t) = (p_3 - p_{amb}) \left(1 - \frac{t - t_{II}}{t_{III} - t_{II}}\right) \quad (3.5.2)$$

$$\rho(t) = \rho_3 \left(\frac{p(t)}{p_3}\right)^{\frac{1}{\gamma_2}} \quad (3.5.3)$$

$$T(t) = \left(\left(\frac{p_3(t)}{p_3}\right)^{\frac{\gamma_2-1}{\gamma_2}} T_3 \right) \quad (3.5.4)$$

The time variable t , in the above expressions is varied from t_{II} to t_{III} , where $t_{II} = 1.45$ ms and $t_{III} = 2.6$ ms. When plotted with respect to time, the pressure decay occurs in a linear manner towards the open end of the tube and the pressure of the flow inside the tube is ambient at $t_{III} = 2.6$ ms.

3.5.2 Final Conditions of Blow Down Process

$$T = 2327.29 \text{ K}$$

$$\rho = 0.11 \frac{\text{kg}}{\text{m}^3}$$

$$p = 1 \text{ atm}$$

The variation in the properties during the rarefaction time period $t_{II} \leq t \leq t_{III}$ is plotted.

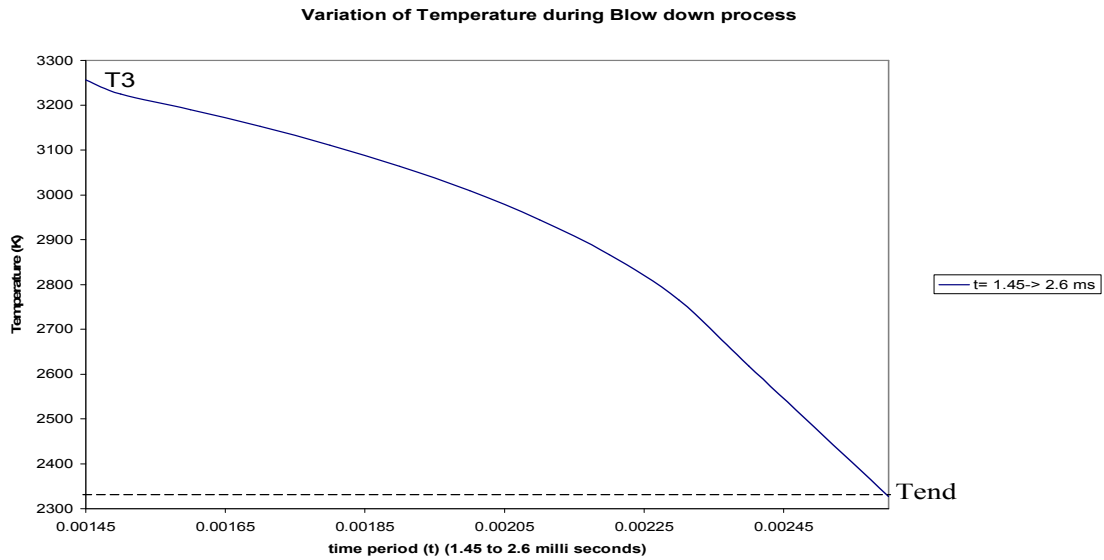


Fig 3.10 Variation in Temperature During Blow Down process

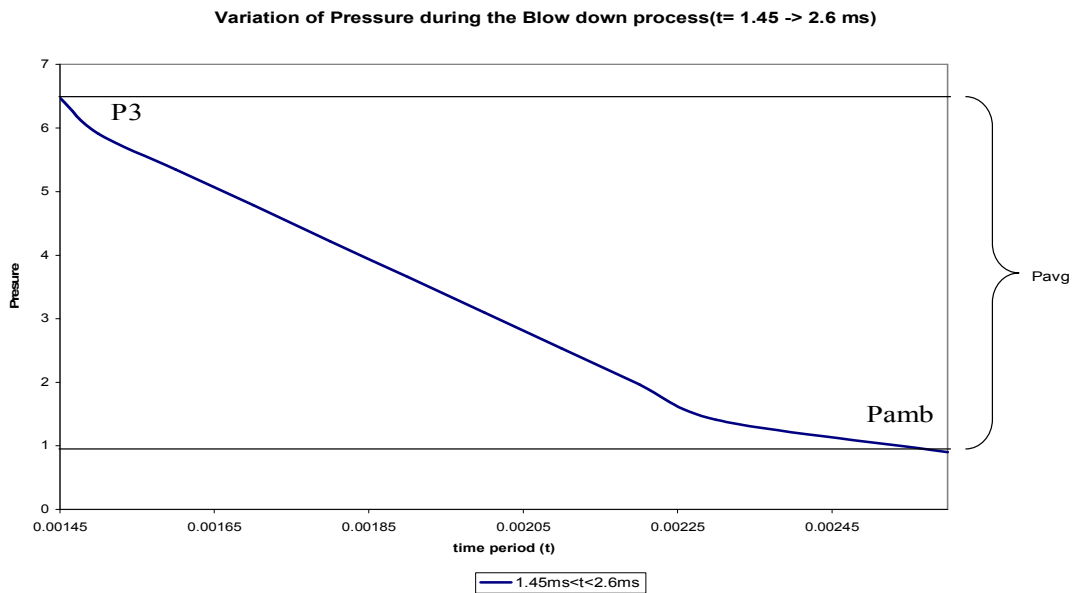


Fig 3.11 Variation in Pressure During Blow Down Process

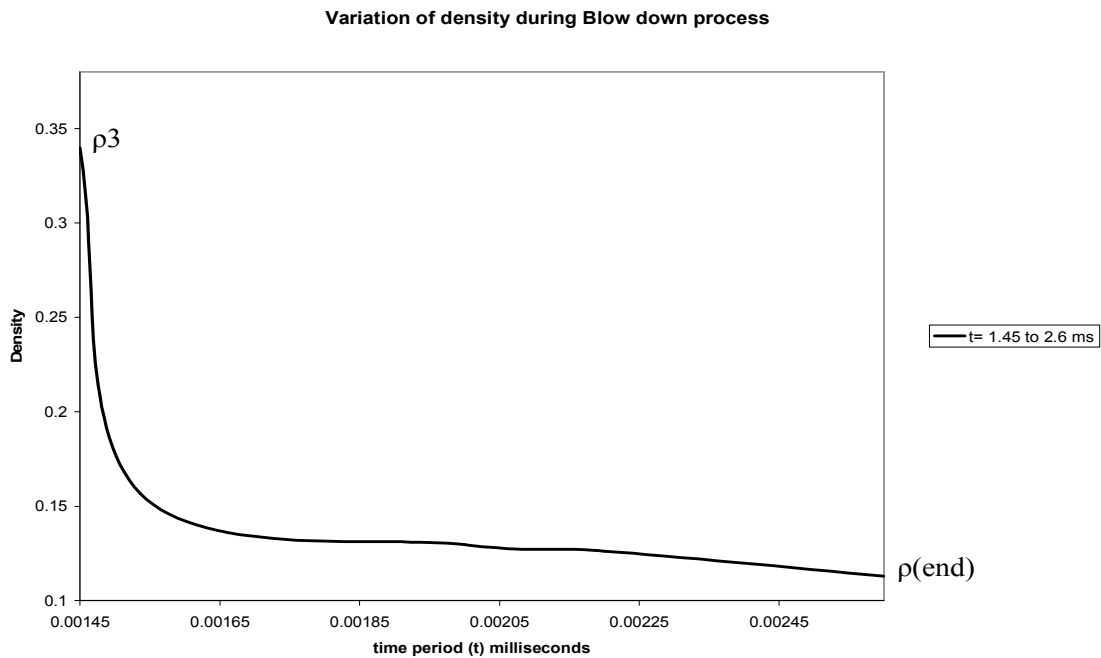


Fig 3.12 Variation in Density During Blow Down Process

From the plots during the Blow down process, the values of pressure and density after the process are almost equal to the initial ambient conditions. However, the temperatures still remain a much higher value and do not reach the ambient conditions.

3.5.3 Average Conditions of Flow During Blow Down Process

$$\bar{T} = 2960.84 \text{ K}$$

$$\bar{p} = 3.65 \text{ atm}$$

$$\bar{\rho} = 0.17 \frac{\text{kg}}{\text{m}^3}$$

3.6 Purging Process

The values of the thermodynamic properties at the end of the purging process are assumed to be ambient as high velocity air is being pumped into the detonation tube to

scavenge the tube before the filling process and also to cool the tube after the high temperature processes that take place before purge.

3.6.1 Initial Conditions of Purging Process

$$T = 2327.29 \text{ K}$$

$$\rho = 0.11 \frac{\text{kg}}{\text{m}^3}$$

$$p = 1 \text{ atm}$$

The purging time as explained in chapter 1 is expressed as $t_{\text{purge}} = \frac{x_L}{V_{\text{fill}}} = 0.02 \text{ s}$. It is

assumed that after the purging process, the conditions inside the detonation chamber are ambient as high velocity air cools the detonation tube. Hence the final conditions inside the tube are ambient given by

3.6.2 Final Conditions of Purging Process

$$T = 300 \text{ K}$$

$$p = 1 \text{ atm}$$

$$\rho = 1.16 \frac{\text{kg}}{\text{m}^3} (\text{air})$$

The following figures outline the profiles of the conditions of the flow for all the properties of the flow starting from detonation process up to purging. The Temperature pressure and Density profiles are plotted with respect to the distance or the length of the detonation tube.

Variation of Pressure along the length of the detonation tube for one cycle of operation

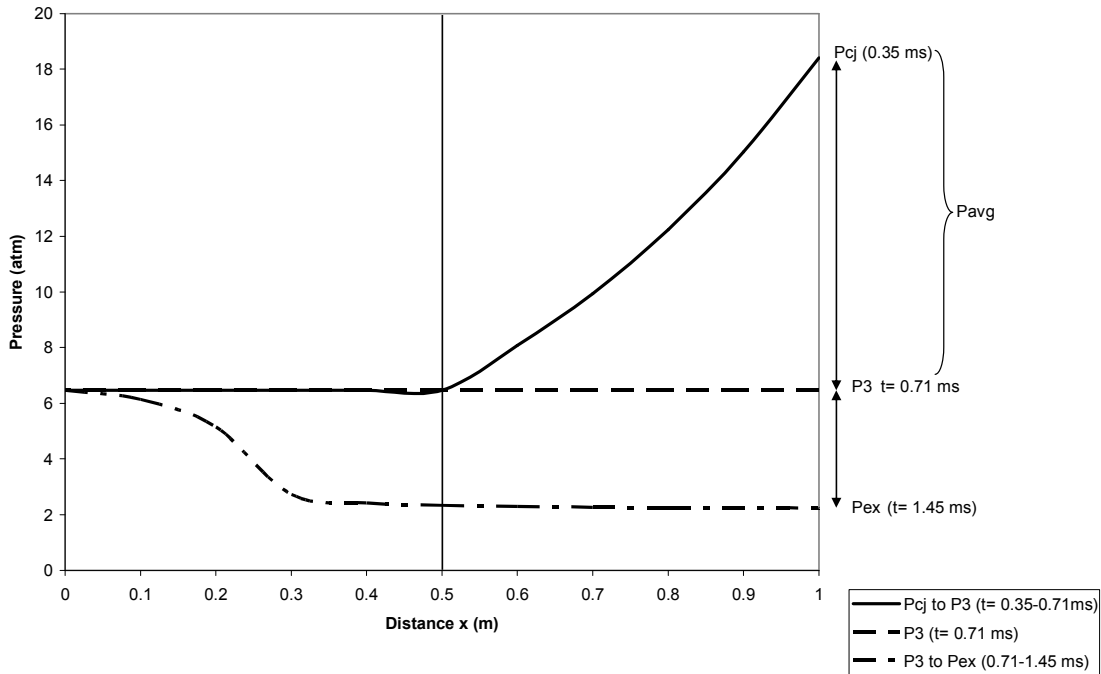


Fig 3.13 Pressure Variation for Taylor Wave and Reflection Processes

In the above plot, it can be clearly observed that the pressure after CJ detonation p_{cj} reduces gradually up to the mid section of the detonation tube. Beyond the mid section, the pressure becomes the end wall pressure after $t=0.71ms$. During the reflection process, the pressure decays from p_3 to p_{ex} which is the end condition of reflection.

Ultimately during the blow down process as shown Fig 3.11 the pressure from p_3 decays linearly to p_{amb} which is approximately equal to $1 atm$.

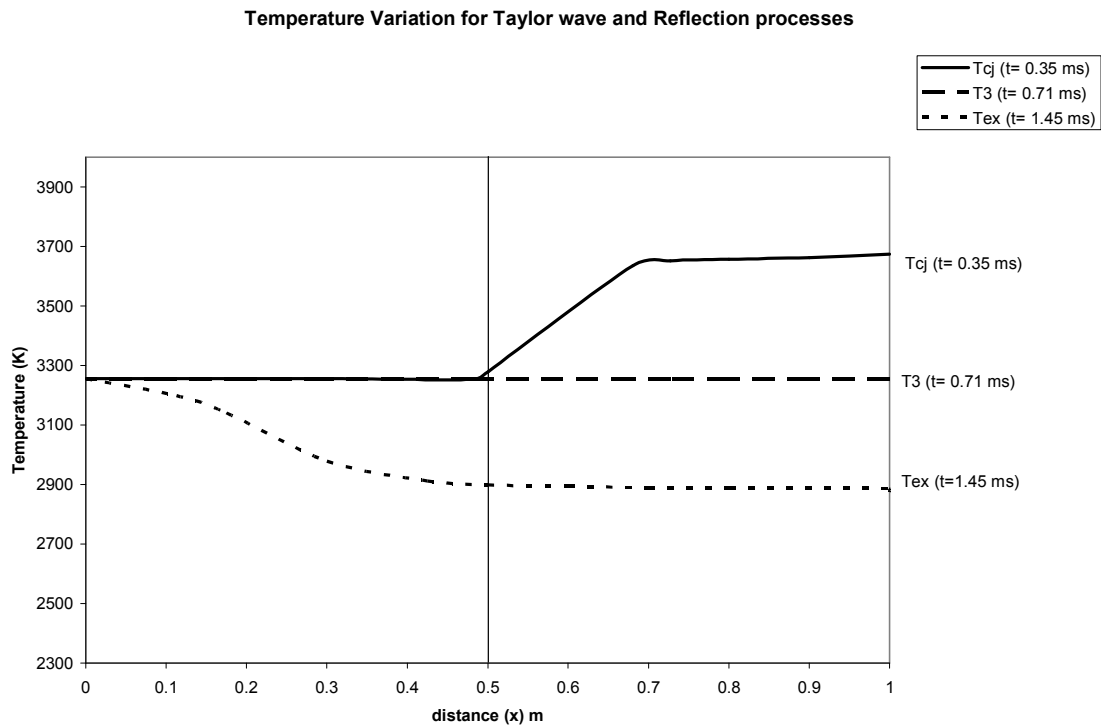


Fig 3.14 Pressure Variation for Taylor Wave and Reflection Processes

The temperature distribution follows the same variation as in the case of pressure. The temperature decays from a high value of T_{cj} up to the mid section of the detonation tube. Beyond the mid section of the tube, it reaches the end wall temperature T_3 and remains constant until $t = 0.71 \text{ ms}$. During reflection; it decays to T_{ex} as represented on the graph. However after the blow down process from fig 3.10, the temperature inside the detonation chamber is still very high and does not reach ambient conditions like in the case of pressure until the tube is scavenged during the purge process. The values for all processes are tabulated as shown in the following table 3.1.

Table 3.1 Average Thermodynamic Properties During Each Process

| Process | Average Temperature(K) | Average Pressure (atm) | Average Density ($\frac{kg}{m^3}$) |
|-----------------------|--|--|--|
| Filling | 300 | 1 | 0.48 |
| CJ Detonation | 3297.89 | 7.92 | 0.40 |
| Taylor Rarefaction | 3256.48 | 6.47 | 0.34 |
| Reflected Rarefaction | 3045.08 | 4.04 | 0.22 |
| Blow Down | 2960.84 | 3.65 | 0.17 |
| Purging Process (air) | 300 | 1.0 | 1.16 |

CHAPTER 4

CALCULATION OF HEAT DISSIPATED FOR ONE CYCLE OF OPERATION

The energy expression for an unsteady flow process is given by equation (1.4.6) to be

$$Q = (mh_t)_e - (mh_t)_i + (m_2u_{t2} - m_1u_{t1}) \quad (4.1)$$

4.1 Application of Energy Expression to The Pulse Detonation Engine

The various processes that take place in the operation of the pulsed detonation cycle are

1. Filling Process
2. CJ Detonation Process
3. Taylor Rarefaction Wave Process
4. Reflected Rarefaction Wave Process
5. Blow Down Process
6. Purging Process

The inlet values of the hydrogen and oxygen mixture that is pumped into the detonation tube with a design velocity of 50 m/s are pressure $(p_i) = 1 \text{ atm}$,

Temperature $(T_i) = 300 \text{ K}$ and density $(\rho_i) = 0.488 \frac{\text{kg}}{\text{m}^3}$. The volume $\pi r^2 x_L = 0.00784$

m^3 for a detonation tube of 0.05 m radius and 1 m length. Also the geometry of the

detonation tube is assumed to be uniform throughout and hence

$V_i = V_e = V = 0.000784 \text{ m}^3$. The surface area of the detonation tube $A = 2\pi r x_L =$

0.314 m^2 .

Also $C_v = \frac{R}{\gamma_2 - 1}$, $C_p = \frac{\gamma_2 R}{\gamma_2 - 1}$ where $R = 0.573 \frac{kJ}{kg.K}$ and $\gamma_2 = 1.128$ (from table 2.1)

and hence $C_v = 4.775 \frac{kJ}{kg.K}$ and $C_p = 5.348 \frac{kJ}{kg.K}$. The values of C_v and C_p calculated

in this section are used in the heat analysis during the detonation process until the purging process. For calculations during the filling process, the values of C_p and C_v are obtained from literature for hydrogen at 300 K .

4.1.1 Filling Process

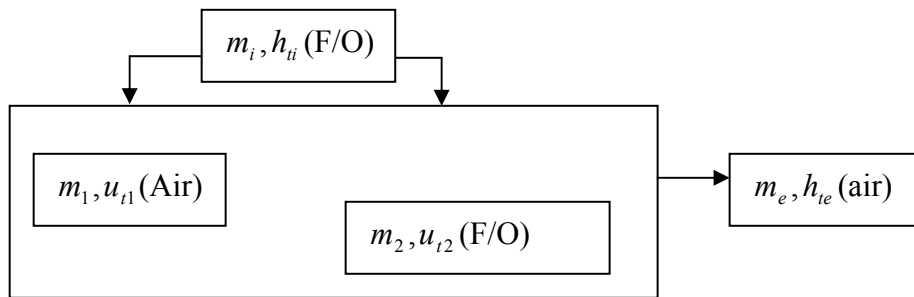


Fig 4.1 Detonation Tube During Filling Process

As depicted in the above figure, during this process, the fuel air mixture is pumped into the detonation tube which in turn forces the air present inside the tube towards the open end of the tube. The mass of the fuel-air mixture pumped into the tube is m_i and the mass of air which is forced out of the tube is m_e . The initial conditions inside the tube are the properties of ambient air and the final conditions are those of the fuel-air mixture since at the end of the filling process, the tube is completely filled with the fuel-air mixture. Hence Eq 4.1 can be rewritten as

$Q = m_e h_{te} - m_i h_{ti} + m_2 u_2 - m_1 u_1$, where

$$m_e h_{te} = \left[(\rho_{air} V) \left(C_p T_e + \frac{v_e^2}{2} \right) \right] \quad (4.1.1)$$

$$m_i h_{ti} = \left[(\rho_{F/O} V) \left(C_p T_i + \frac{v_i^2}{2} \right) \right] \quad (4.1.2)$$

$$m_1 u_1 = (\rho V)_{air} (C_v T_2)_{air} \quad (4.1.3)$$

$$m_2 u_2 = (\rho V)_{F/O} (C_v T_2)_{F/O} \quad (4.1.4)$$

C_p and C_v for Hydrogen at 300 K = $14.307 \frac{kJ}{kg.K}$, $10.183 \frac{kJ}{kg.K}$. Similarly for

air, $C_p = 1.005 \frac{kJ}{kg.K}$, $C_v = 0.718 \frac{kJ}{kg.K}$. The internal energy in the above expression is

calculated using the expression $u = C_v T$. Also in this case, $m_i = m_2$ as the mass of the fuel pumped into the tube is the final mass that is stored in the system before detonation and $m_e = m_1$. The inlet velocity $v_i = 50 \frac{m}{s}$. It is assumed that the inlet and the exit

velocities are equal $v_i = v_e$. All the properties of the fuel and air are substituted into the equations 4.1.1 to 4.1.4 and the energy transferred from the control volume is calculated. The following table outlines the properties of the air and fuel air mixture during the filling process and the heat dissipated from the system during the filling process.

Table 4.1 Thermodynamic Properties During the Filling Process

| | | | | |
|-------------------------|------------------------|---------------|---------------|-------------------|
| $m_i = m_2$ (F/O) | ρ_i (F/O) | $V_i = V_e$ | v_i | $m_e = m_1$ (air) |
| 0.003832 kg | $0.488 \frac{kg}{m^3}$ | $0.00784 m^3$ | 50 m/s | 0.00917 kg |
| ρ_e (air) | $T_i = T_2$ | $T_1 = T_e$ | $t_{filling}$ | Q (kJ) |
| $1.1614 \frac{kg}{m^3}$ | 300 K | 300 K | 0.02 s | -8.74 |

The heat transferred from the detonation tube is calculated to be -8.74043 kJ. The time taken by this process is 0.02 s. Ultimately, the heat dissipation from the detonation tube during the filling process is calculated to be

$$\dot{Q} = \frac{Q(kJ)}{t_{filling}(s)} = \frac{-8.74 kJ}{0.02 s} = -437 \frac{kJ}{s} = -437 KW, \text{ which is equal to } -0.437 MW.$$

4.1.2 CJ Detonation Process

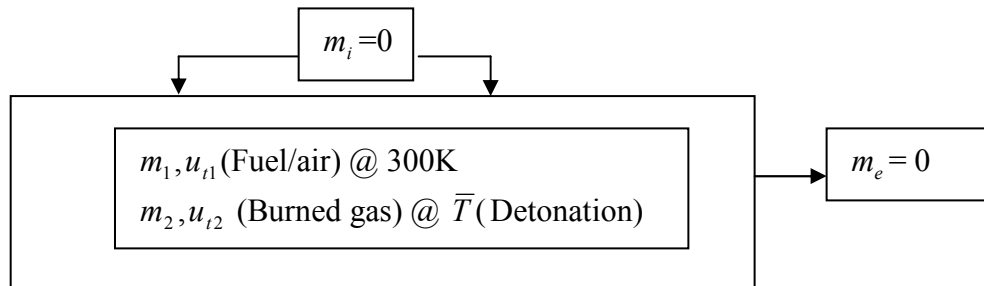


Fig 4.2 Detonation Tube During Detonation Process

Considering Eq 4.1, $Q = (mh_t)_e - (mh_t)_i + (m_2 u_{t2} - m_1 u_{t1})$

As shown in the above figure, during this phase, the inlet and exit terms are completely neglected in equation 4.1 and hence the energy equation can be rewritten as $Q = (m_2 u_{t2} - m_1 u_{t1})$. Also since there is no change in the mass inside during the detonation phase, the differential change in mass with respect to time is zero and hence $m_2 = m_1$. The above energy expression can be rewritten as $Q = m(u_{t2} - u_{t1})$, where $u_{t2} = C_V \bar{T} + \frac{v_2^2}{2}$, where $\bar{T} = \text{avg}(T_{c1} \text{ to } T_3)$ and $u_{t1} = C_V T_1 + \frac{v_1^2}{2} + h_{PR}$. In these two expressions, $v_2, v_1 = 0$ as the mixture is assumed to be at rest before detonation and hence kinetic energies during the process are neglected and h_{PR} for hydrogen fuel is $42,800 \frac{kJ}{kg}$. The mass m inside the detonation tube is 0.003832 kg (from filling process). Internal energy $u_{t1} = u_{t2}$ (filling process) + $h_{PR} = 45854.9 \frac{kJ}{kg}$ and $u_{t2} = C_V T_2 = 15747.45 \frac{kJ}{kg}$. The following table outlines the various properties of the fuel (hydrogen) oxide mixture before and after detonation. The values of the average temperatures during filling and detonation are obtained from Table 3.1.

Table 4.2 Thermodynamic Properties During CJ Detonation Process

| m_i (kg) | m_e (kg) | T_1 (K) | \bar{T} (K) | m (kg) | $C_v @ T_1$ |
|-------------|------------------------|------------------------|------------------------|----------|----------------|
| 0 | 0 | 300 | 3297.896 | 0.003832 | 10.183 |
| $C_v @ T_2$ | $u_{t1} \frac{kJ}{kg}$ | $u_{t2} \frac{kJ}{kg}$ | $h_{PR} \frac{kJ}{kg}$ | Q (kJ) | \dot{Q} (MW) |
| 4.775 | 45854.9 | 15747.45 | 42800 | -115.391 | -326.886 |

The heat transferred from the detonation tube in this process is calculated to be -115.391 kJ . The detonation time is 0.00035 seconds. Ultimately the heat dissipation rate during this process \dot{Q} is calculated to be

$$\dot{Q} = \frac{Q(kJ)}{t_{filling}(s)} = \frac{-115.391 kJ}{0.000353 s} = -326886 \frac{kJ}{s} = -326886 KW \text{ which is equivalent to } -326 MW .$$

4.1.3 Taylor Rarefaction Wave Process

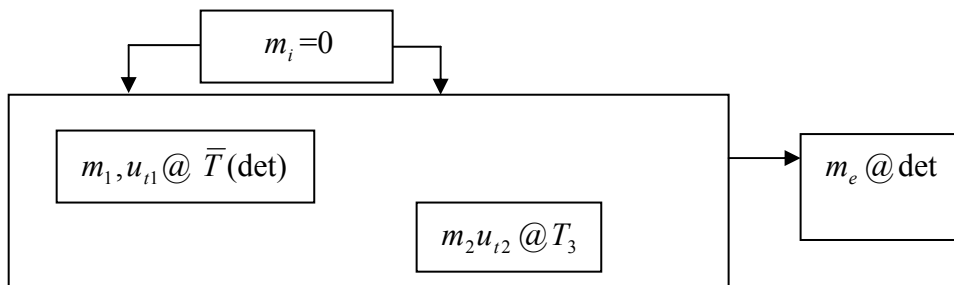


Fig 4.3 Detonation Tube During Taylor Wave Process

Considering Eq 4.1, $Q = (mh_t)_e - (mh_t)_i + (m_2u_{t2} - m_1u_{t1})$

This process is assumed to be taking place instantaneously after the detonation process. Similar to the above process, the inlet terms in the above expression are neglected and the above expression is rewritten as $Q = mh_{te} + (m_2u_{t2} - m_1u_{t1})$. In this equation, the exit terms are those of the burned gases which leave the detonation tube from the open end. The same process is repeated as in the case of detonation, the only difference being the presence of the exit term in the energy equation. The exit mass $m_e = m_1 - m_2$. During this process,

$$m_e = m_1 - m_2 \quad (4.1.5)$$

$$h_{te} = C_p T_e + \frac{v_e^2}{2} \quad (4.1.6)$$

$$m_1 = m_{\text{det}} \quad (4.1.7)$$

Also $u_{t2} = u_{t2}$ (detonation), as this process is assumed to be taking simultaneously with

the CJ detonation process, $u_{t1} = C_v T_1 + \frac{v_1^2}{2}$, where $v_1 = \frac{\dot{m}_1}{\rho_1 A_1} = 36 \frac{m}{s}$.

The following table outlines the various properties of the fuel air mixture during this process.

Table 4.3 Thermodynamic Properties During Taylor Rarefaction Wave Process

| $m_1 = m(\text{det})(kg)$ | $m_e (kg)$ | $C_v, C_p (\frac{kJ}{kg.K})$ | $m_2 (kg)$ | $T_e = T_3 (K)$ |
|---------------------------|------------|------------------------------|-------------------|-------------------|
| 0.003832 | 0.001109 | 4.775, 5.348 | 0.002723 | 3256.489 |
| $T_1 (K)$ | $T_2 (K)$ | $m_e h_{te} (kJ)$ | $m_1 u_{t1} (kJ)$ | $m_2 u_{t2} (kJ)$ |
| 3297.896 | 3256.489 | 19.43617 | 62.97092 | 42.88291 |

The heat transferred from the detonation tube in this process is calculated to be - 0.65184 kJ . The time is 0.00071 seconds. Ultimately the power dissipated or the heat

dissipation rate during this process \dot{Q} is calculated to be $\dot{Q} = \frac{Q(kJ)}{t_{filling}(s)} = \frac{-0.65 kJ}{0.00071s}$

$= -915.49 \frac{kJ}{s} . = -915.49 KW$, which is equal to - 0.915 MW .

4.1.4 Reflected Rarefaction Wave Process

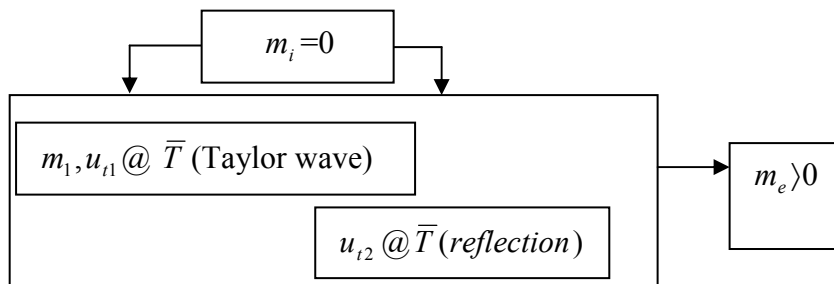


Fig 4.4 Detonation Tube During Reflected Rarefaction Process

Considering $Q = (mh_t)_e - (mh_t)_i + (m_2u_{t2} - m_1u_{t1})$

During this process, a reflected wave travels from the open end to the closed end of the detonation tube. The inlet terms in the energy balance equation are neglected as there is no fuel intake into the system. The energy balance equation for this process is thus given as $Q = (mh_t)_e + (m_2u_{t2} - m_1u_{t1})$. During this process, high temperature gases exit the tube and hence the exit terms cannot be neglected. Similar to the above processes, the thermodynamic properties at state 1 during this process are the final properties during the Taylor rarefaction process. The exit velocities during this process, are calculated using the mass flow parameter relation which is expressed as

$$\dot{m}_e = \rho_e A_e v_e, \quad v_e = \frac{\dot{m}_e}{\rho_e A_e}, \quad \& \quad v_2 = \frac{\dot{m}_e}{\rho_2 A_2} \quad \text{where } m_e = \rho_e V_e \quad (4.1.8)$$

$$m_2 = \rho_2 V_2 \quad (4.1.9)$$

$$u_{t2} = C_v T_2 + \frac{v_2^2}{2} \quad (4.1.10)$$

$$u_{t1} = u_{t2} \text{ (Taylor rarefaction process)}$$

Table 4.4 Thermodynamic Properties During Reflected Rarefaction Process

| | | | | |
|---|------------|----------------------------------|-------------------|-------------------|
| $m_1 = m_2$ (Taylor process (kg)) | m_e (kg) | C_v, C_p ($\frac{kJ}{kg.K}$) | m_2 (kg) | T_e (K) |
| 0.002723 | 0.000925 | 4.775, 5.348 | 0.001798 | 2874.351 |
| T_1 (K) | T_2 (K) | $m_e h_{te}$ (kJ) | $m_1 u_{t1}$ (kJ) | $m_2 u_{t2}$ (kJ) |
| 3256.489 | 3045.081 | 15.17216 | 42.88291 | 26.41453 |

The heat transferred from the detonation tube in this process is calculated to be - 1.29662 kJ . The time is 0.00145 seconds. Ultimately the power dissipated or the heat

dissipation rate during this process \dot{Q} is calculated to

$$\text{be } \dot{Q} = \frac{Q(kJ)}{t_{filling}(s)} = \frac{-1.29 kJ}{0.00145 s} = -889 \frac{kJ}{s} = -889 KW = -0.889 MW.$$

4.1.5 Blow Down Process

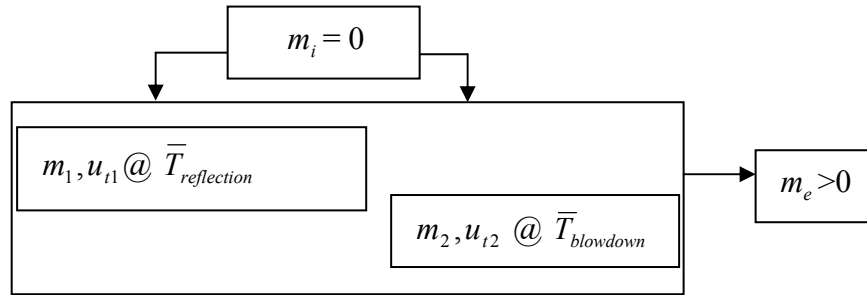


Fig 4.5 Detonation Tube During Blow Down Process

Considering Eq 4.1, $Q = (mh_t)_e - (mh_t)_i + (m_2u_{t2} - m_1u_{t1})$. The reflected rarefaction wave after traversing from the open end to the closed end of the detonation tube reflects back to the open end after colliding with the closed end of the tube. Similar to the above process, the inlet terms in the above expression are neglected and the above expression is rewritten as $Q = (mh_t)_e + (m_2u_{t2} - m_1u_{t1})$. The internal energy

$$u_{t1} = C_v T_1 + \frac{v_1^2}{2} = 15595.92 \frac{kJ}{kg} \text{ and } u_{t2} = C_v T_2 + \frac{v_2^2}{2} = 14184.25 \frac{kJ}{kg}.$$

Table 4.5 Thermodynamic Properties During Blow Down Process

| $m_1 (kg)$ | $m_e (kg)$ | $C_v, C_p (\frac{kJ}{kg \cdot K})$ | $m_2 (kg)$ | $T_e (K)$ |
|------------|------------|------------------------------------|-------------------|-------------------|
| 0.001798 | 0.00043 | 4.775, 5.348 | 0.0013686 | 2327.29 |
| $T_1 (K)$ | $T_2 (K)$ | $m_e h_{te} (kJ)$ | $m_1 u_{t1} (kJ)$ | $m_2 u_{t2} (kJ)$ |
| 3256.489 | 2960.843 | 7.215483 | 27.99876 | 19.41327 |

The heat transferred from the detonation tube in this process is calculated to be - 1.37001 kJ . The time is 0.0026 seconds. Ultimately the power dissipated or the heat dissipation rate during this process \dot{Q} is calculated to

$$\text{be } \dot{Q} = \frac{Q(kJ)}{t_{filling}(s)} = \frac{-1.37 kJ}{0.0026 s} = -526. \frac{kJ}{s} = -526 KW = -0.526 MW.$$

4.1.6 Purging Process

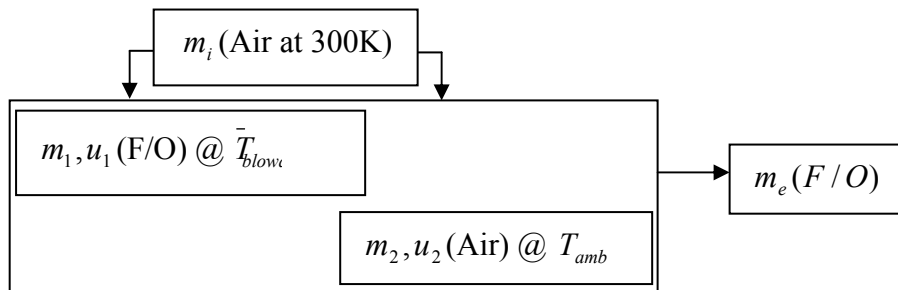


Fig 4.6 Detonation Tube During Purging Process

The main aim of implementing this process immediately after the blow down process is to further cool the detonation tube. Ambient air is pumped into the tube at certain design velocities which aids in bringing the temperature inside the detonation chamber from a very high value to an ambient value. Also, this process can also be used to scavenge the tube as the high velocity air forces all the burned combustion products which are left over inside the tube. In the absence of this process, residual high temperature combustion products would auto-ignite the fuel as it enters the detonation tube and ultimately lead to deflagration. The energy balance expression in this case is similar to that of the filling process, the only difference being that ambient air is pumped into the

tube replacing fuel/oxidizer mixture in the filling process. The energy balance expression is expressed as

$$Q = m_e h_{te} - m_i h_{ti} + m_2 u_2 - m_1 u_1, \text{ where}$$

$$m_e h_{te} = \left[(\rho_{F/O} V) \left(C_p T_e + \frac{v_e^2}{2} \right) \right] \quad (4.1.11)$$

$$m_i h_{ti} = \left[(\rho_{air} V) \left(C_p T_i + \frac{v_i^2}{2} \right) \right] \quad (4.1.12)$$

$$m_2 u_{t2} = (\rho V)_{air} \left(C_v T_2 + \frac{v_2^2}{2} \right)_{air} \quad (4.1.13)$$

$$m_1 u_{t1} = (\rho V)_{F/O} \left(C_v T_1 + \frac{v_1^2}{2} \right)_{F/O} \quad (4.1.14)$$

The properties at the inlet are the properties of the ambient air at 300 Kelvin temperature and hence the mass at the inlet is expressed as $m_i = \rho_i V_i$, where

$\rho_i = 1.1614 \frac{kg}{m^3}$ and $V_i = 0.00785 m^3$ and the inlet mass is calculated to be

$0.009121 kg$. The inlet enthalpy is calculated using the relation $h_{ti} = C_p T_i + \frac{v_i^2}{2}$ and

calculated to be $1551.5 \frac{kJ}{kg}$. The properties at state 1 are obtained during the blow down

process.

Table 4.6 Thermodynamic Properties During Purging Process

| | | | |
|-------------------|------------------------|-------------|----------------------|
| $m_i = m_2$ (air) | $V_i = V_e$ | $v_i = v_e$ | $m_e = m_1$ (F/O) kg |
| 0.009121 kg | 0.00784 m ³ | 50 m/s | 0.001369 |
| $T_i = T_2$ (K) | $T_1 = T_e$ (K) | t (s) | Q (kJ) |
| 300 | 2960.843 | 0.02 | -8.15093 |

The heat transferred from the detonation tube in this process is calculated to be -8.15093 kJ. The time is 0.02 seconds. Ultimately the power dissipated or the heat dissipation rate during this process \dot{Q} is calculated to be

$$\dot{Q} = \frac{Q(kJ)}{t_{filling}(s)} = \frac{-8.15093 kJ}{0.02 s} = -407 \frac{kJ}{s} = -407 KW = -0.407 MW.$$

The total heat dissipated from the detonation tube for one cycle of operation $Q = -135.6$ kJ. The heat dissipation rate for one cycle of operation

$$\dot{Q} = \frac{Q}{t_{cycle}} = \frac{Q}{(t_{fill} + t_{det} + t_{Taylor} + t_{reflection} + t_{Blowdown} + t_{purge})} = \frac{-135.6}{0.045113} = -3007.3 MW.$$

CHAPTER 5

CALCULATION OF WALL TEMPERATURES USING GREEN'S FUNCTIONS

The objective of this section is to present procedures for determination of temperature within the walls of the detonation chamber. The detonation tube has an inner radius of r_i and an outer radius of r_o , as shown in the following figure 5.1. The detonation tube is assumed to be made up of Copper. The surface of this enclosure, at $r = r_o$ location, is being cooled by a coolant which is water in this case. The inner walls of the detonation tube face varying temperatures depending on the process taking place.

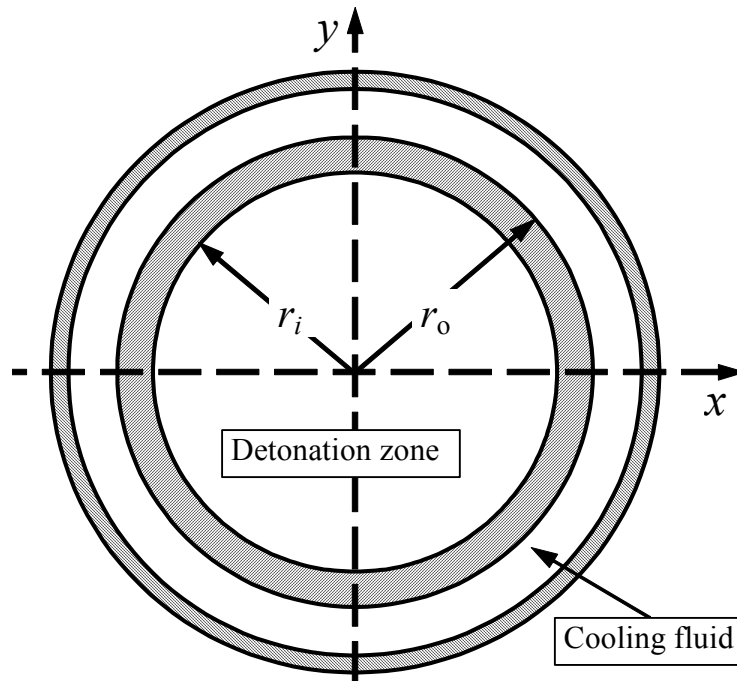


Fig. 5.1 Cross Sectional View of the Detonation Tube

For a cylinder as shown in the above Fig. 5.1 with an inner radius of r_i which is initially at room temperature and due to a thermodynamic processes occurring inside it, rapid changes in temperature takes place across its surface due to both conduction through the walls and also due to convection due to the flow of coolant inside it. The type of convection employed in this case is forced convection as the coolant is pumped with a certain velocity to dissipate the heat from the walls of the cylinder. An estimation of the temperature solution may be obtained for the time dependence of the radial temperature distribution.

There are two solutions available for this kind of problem. The first one being the transient analysis solution and the other being the steady state solutions. The following are the assumptions in this analysis.

1. Thermo- physical properties are independent of temperature.
2. Axial conduction in along the walls of the detonation chamber is neglected.
3. The arriving heat flux $\dot{q} = \frac{\dot{Q} (W)}{A(m^2)}$, where \dot{Q} is obtained from Table 5.1 for each process and $A = 0.3614 m^2$.
4. Heat flux is considered to be uniform during the detonation period.

5.1 Transient Analysis Solution of Heat Conduction Through Hollow Cylinders

The solution of the temperature distribution for the above mentioned case using Green's Functions (adapted from Ref. 5) for a finite body with homogeneous boundary conditions as

$$T(r, t) = 2\pi \int_{r'=r_i}^{r_o} G(r, t | r', 0) F(r') r' dr' + \frac{2\pi\alpha}{k} \int_{\tau=0}^t \int_{r'=r_i}^{r_o} G(r, t | r', \tau) g(r', \tau) r' dr' d\tau \quad (5.2.1)$$

In the above equation, the non zero initial temperature distribution $F(x')$ is equated to zero as in the following analysis, it is assumed that the reduced surface temperature $T - T_\infty$ is a zero initially during the beginning of the process and hence the above equation is rewritten as

$$T(x, t) - T_\infty = \frac{2\pi\alpha}{k} \int_{\tau=0}^t \int_{r'=r_i}^{r_o} G(r, t | r', \tau) g(r', \tau) r' dr' d\tau \quad (5.1.2)$$

In the above equation, $g = \delta(r' - a)\dot{q}$ and $G(r, t | r', \tau)$ is the Green's Function solution for a hollow cylinder. The green's function satisfies the homogenous boundary

conditions which is described by the conditions $\frac{\partial G}{\partial r} = 0$ at $r = r_i$, $k \frac{\partial G}{\partial r} + hG = 0$ at

$r = r_o$ given by

$$G(r, t | r', \tau) = \frac{\pi}{4a^2} \sum_{m=1}^{\infty} e^{-\beta_m^2 \alpha (t-\tau) / a^2} \frac{\beta_m^2 J_1^2(\beta_m)}{(B^2 + \beta_m^2) J_1^2(\beta_m) - V_o^2} \quad (5.1.3)$$

$$\left[S_o J_o\left(\beta_m \frac{r}{r_i}\right) - V_o Y_o\left(\beta_m \frac{r}{r_i}\right) \right] \left[S_o J_o\left(\beta_m \frac{r'}{r_i}\right) - V_o Y_o\left(\beta_m \frac{r'}{r_i}\right) \right]$$

where, $S_o = -\beta_m Y_1\left(\beta_m \frac{r_o}{r_i}\right) + B Y_o\left(\beta_m \frac{r_o}{r_i}\right)$, $V_o = -\beta_m J_1\left(\beta_m \frac{r_o}{r_i}\right) + B J_o\left(\beta_m \frac{r_o}{r_i}\right)$, \dot{q} the

heat flux during each process and r_i is the inner radius of the detonation tube.

Substituting all the expressions into the above equation, the temperature distribution is expressed as

$$T_i - T_\infty = \frac{2\pi\alpha}{k} \int_{\tau=0}^t \int_{r'=a}^{r'_0} G(r, t : r', \tau) \delta(r' - r_i) \dot{q} r' dr' \quad (5.1.4)$$

$$T_i - T_\infty = \frac{2\pi\alpha}{k} \int_{\tau=0}^t G(r, t : r', \tau) \dot{q}_i d\tau \quad (5.1.5)$$

Now substituting the value of the Green's Functions expression as given by equation 5.1.3 into 5.1.5,

$$\begin{aligned} T_i - T_\infty &= \frac{2\pi r \alpha}{k} \int_{\tau=0}^t \frac{\pi}{4a^2} \sum_{m=1}^{\infty} e^{-\beta_m^2 \alpha (t-\tau) / r_i^2} \frac{\beta_m^2 J_1^2(\beta_m)}{(B^2 + \beta_m^2) J_1^2(\beta_m) - V_o^2} \\ &\times \left[S_o J_o\left(\beta_m \frac{r}{r_i}\right) - V_o Y_o\left(\beta_m \frac{r}{r_i}\right) \right] \left[S_o J_o\left(\beta_m \frac{r'}{r_i}\right) - V_o Y_o\left(\beta_m \frac{r'}{r_i}\right) \right] \dot{q}_i d\tau \end{aligned} \quad (5.1.6)$$

That can be written as

$$\begin{aligned} T_i - T_\infty &= \frac{2\pi r \alpha}{k} \frac{\pi}{4r_i^2} \sum_{m=1}^{\infty} e^{-\beta_m^2 \alpha t / r_i^2} \left(\int_{\tau=0}^t e^{\beta_m^2 \alpha \tau / r_i^2} d\tau \right) \frac{\beta_m^2 J_1^2(\beta_m)}{(B^2 + \beta_m^2) J_1^2(\beta_m) - V_o^2} \\ &\times \left[S_o J_o\left(\beta_m \frac{r}{r_i}\right) - V_o Y_o\left(\beta_m \frac{r}{r_i}\right) \right] \left[S_o J_o\left(\beta_m \frac{r'}{r_i}\right) - V_o Y_o\left(\beta_m \frac{r'}{r_i}\right) \right] q_i d\tau \end{aligned} \quad (5.1.7)$$

Ultimately, the temperature expression for transient heat conduction through hollow cylinders is expressed as

$$\begin{aligned} \frac{k(T - T_\infty)}{q_i r_i} &= \frac{\pi^2}{2} \sum_{m=1}^{\infty} \left[1 - e^{-\beta_m^2 \alpha t / r_i^2} \right] \frac{\beta_m^2 J_1^2(\beta_m)}{(B^2 + \beta_m^2) J_1^2(\beta_m) - V_o^2} \\ &\times \left[S_o J_o\left(\beta_m \frac{r}{r_i}\right) - V_o Y_o\left(\beta_m \frac{r}{r_i}\right) \right] \left[S_o J_o\left(\beta_m \frac{r'}{r_i}\right) - V_o Y_o\left(\beta_m \frac{r'}{r_i}\right) \right] \end{aligned} \quad (5.1.8)$$

Utilizing the above equation, the local values of the wall temperatures during each process can be obtained. In the above expression, k is the thermal conductivity of copper which is $400 \frac{W}{mK}$, r_i is the inner radius of the water jacket (m), q_i is the wall heat flux during each process $q_i = \frac{\dot{Q}}{A} \left(\frac{W}{m^2} \right)$, t_i the time taken by each process. The following table 5.1 outlines the time period, the average temperatures and the heat dissipation rate during each process.

Table 5.1 Time period, Temperatures and Heat Dissipated During Each Process

| Process | Time period(<i>ms</i>) | Temperatures T_g (<i>K</i>) | Heat Dissipation rate (<i>MW</i>) |
|--------------------|--------------------------|---------------------------------|-------------------------------------|
| Filling | 20 | 300 | -0.43 |
| CJ Detonation | 0.35 | 3297.89 | -326 |
| Taylor rarefaction | 0.71 | 3256.48 | -0.91 |
| Reflection | 1.45 | 3045.08 | -0.88 |
| Blow down | 2.9 | 2960.84 | -0.52 |
| Purging | 20 | 300 | -0.40 |

The equation (5.1.8) is then applied to obtain the value of wall temperatures during various processes that take place during the pulse detonation cycle. Due to the complexity of calculations involved, the entire expression is given as an input to Mathematica, which calculates the wall temperatures during each process i.e. filling, detonation, rarefaction and purging. The input data to the Mathematica code in this case is the fuel and oxidizer mixture at ambient conditions. Water is assumed to be flowing around the detonation tube as shown in fig 5.1 at an assumed design velocity $\left(15.24 \frac{m}{s}\right)$.

The nature of the water flowing, i.e. either turbulent or laminar is determined by calculating the Reynolds number which is expressed as $R_{eD} = \left(\frac{\rho v D}{\mu}\right)$, Where, $v =$

$15.24 \frac{m}{s}$, $\rho = 1000 \frac{kg}{m^3}$, D is the hydraulic diameter expressed as $D_o - D_i = 0.28 - 0.14$

$= 0.14$ and μ is the absolute viscosity of the fluid $= 8.55e-4 \frac{N.s}{m^2}$. The Reynolds number

is calculated to be $1.15E+06$, which is greater than the typically assumed value of 10,000 required for turbulent flow and hence the nature of water flowing is completely turbulent. The Nusselt number N_{uD} for turbulent flow in circular tubes (adapted from Ref.5) for a given Prandtl number Pr of 5.83 for water at 300 K and Reynolds number R_{eD} of $1.15E+06$ is calculated to be approximately 500.

1. Velocity V(m/s) which is assumed to be an empirical design value of $15.24 \frac{m}{s}$

2. Thermal conductivity $k_c = 6.2e-01 \frac{W}{mK}$ for water at 300 K

3. Density $\rho = 1000 \left(\frac{kg}{m^3} \right)$ for water which is the coolant in this case,

4. Hydraulic Diameter $D_h = 0.14(m)$

The overall heat transfer coefficient is calculated to be $h = 2190 \frac{W}{m^2K}$.

5.2 Calculation of Wall Temperatures for One Cycle of Operation

The velocity of water flowing through the tubes is kept constant throughout the entire cycle and hence a constant value of heat transfer coefficient is maintained. As shown in fig 5.1, the outer wall of the detonation tube is in contact with the cooling water while the inner walls face the high temperature gases and hence the outer walls are much cooler than the inner walls. The values of T_{w1} and T_{w2} are calculated for each process starting from filling up to purging and then all the obtained values are averaged for the entire cycle time. The input parameters are

1. $h_c = 2190 \frac{W}{m^2K}$,

2. $T_c = T_g$, Where, T_g is given from the table 5.1 for each process and

3. t_p = Time taken for a process obtained from table 5.1 (filling, CJ Detonation, Taylor rarefaction, Reflected rarefaction, Blow down and purging),

$t_{end} = 0.045113s (t_{fill} + t_{det} + t_{Taylor} + t_{reflection} + t_{Blowdown} + t_{purge})$. The energy released is \dot{Q}

in watts and is obtained from Table 5.1 The present analysis is conducted by selecting

two materials namely Copper and Steel (AISI 304).The criteria for selecting two different materials is the behavior of these metals during high temperatures. The thermal conductivity of steel at 300 K is $14.9 \frac{W}{m.K}$ and that of copper is $401 \frac{W}{m.K}$. The value of h_c is maintained constant for all the processes.

5.2.1 Wall Temperatures During Filling Process

The input parameters are $h_c = 2190 \frac{W}{m^2.K}$, $T_g = T_c = 300K$, $r = r_i$, $t_{process} = 0.02 s$, $t_{cyc} = 0.045113 s$. The number of pulses (n_p) in this case is 1 .The thermal conductivity

k for copper at 300 K = $401 \frac{W}{m.K}$ and $\dot{q} = \frac{\dot{Q}}{A}$ where \dot{Q} is obtained from Table 5.1 for

filling process and A is the area of the detonation tube which is equal to $0.314 m^2$. The

differential time period is $\Delta t_1 = \frac{t_p}{20}$ where t_p is the time taken by the filling process. The

average temperature during this process is obtained using the curve fitting techniques and hence the temperatures obtained during the first half of the cycle are added and multiplied by Δt_1 and the remaining temperatures are added together and multiplied

with Δt_2 which is equal to $\frac{t_e - t_p}{20}$. The range of temperatures before and after the

differential time period Δt_1 are neglected as the differential change in temperatures for one cycle is negligible. The values obtained from both the cases are added together and divided by the cycle time is 0.045113 s to obtain the average inner wall temperature

which is 301.865 K . The same procedure is carried out in the calculations of the outer wall temperatures, the only difference being in this case is that $r = r_o$. The outer wall temperature during this process is calculated to be 300 K .

5.2.2 Wall Temperatures During CJ Detonation Process

The initial wall temperature for this process is the final wall temperature after the filling

process. The input parameters are $h_c = 2190 \frac{W}{m^2 K}$, $t_{process} = 0.000353\text{ s}$,

$t_{cyc} = 0.045113\text{ s}$ and thermal conductivity k for copper at $300\text{ K} = 401 \frac{W}{m.K}$ and $\dot{q} = \frac{\dot{Q}}{A}$

where \dot{Q} is obtained from Table 5.1 for CJ detonation process and A is the area of the detonation tube which is equal to 0.314 m^2 . The average wall temperatures obtained during this process $T_{wl} = 316.1316\text{ K}$. In spite of huge energy release during this process, the wall temperatures do not vary much in this process. This can be attributed to the fact that the time taken by this process is very small and also due to the presence of high velocity water cooling the detonation tube on the other side. The high thermal conductivity of copper also plays a vital role in the result of low temperature rise during this process. However if operated for repetitive cycles, the temperatures increase linearly with time. The outer wall temperature during this process is calculated to be 300.01 K .

5.2.3 Wall Temperatures During Taylor Rarefaction Wave Process

The initial wall temperatures are obtained from the final conditions of the detonation process. The input parameters are $h_c = 2190 \frac{W}{m^2 K}$, $t_{process} = 0.00071 s$, $t_{cyc} = 0.045113 s$,

$T_c = T_g = 3256 K$ and thermal conductivity k for copper at $300 K = 401 \frac{W}{m.K}$ and

$\dot{q} = \frac{\dot{Q}}{A}$ where \dot{Q} is obtained from Table 5.1 for Taylor rarefaction process and A is the

area of the detonation tube which is equal to $0.314 m^2$. The same procedure is repeated as in the case of Detonation process and the average wall temperatures during this process are $T_{w1} = 316.22 K$ and $T_{w2} = 300 K$.

5.2.4 Wall Temperatures During Reflected Rarefaction Wave Process

The initial temperatures of the walls are the final temperatures during the Taylor wave process. The input parameters are similar to that of the above processes, the only difference being in the time period and temperatures during this process

$\bar{T} = 3045.081 K$, $t_{process} = 0.00145 s$, $t_{cyc} = 0.045113 s$ and $\dot{q} = \frac{\dot{Q}}{A}$ where \dot{Q} is obtained

from Table 5.1 for reflection process and A is the area of the detonation tube which is equal to $0.314 m^2$. The average wall temperatures during this process are

$T_{w1} = 316.38 K$, $T_{w2} = 300 K$. The wall temperatures produced during this process are

higher when compared with the detonation process due to the fact that the time taken by this process is much higher than detonation process.

5.2.5 Wall Temperatures During Blow Down Process

The input parameters are $h_c = 2190 \frac{W}{m^2 K}$, $T_g = T_c = 2960.843 K$, $t_{process} = 0.0026 s$

$t_{cyc} = 0.045113 s$ and thermal conductivity k for copper at $300 K = 401 \frac{W}{m.K}$ and $\dot{q} = \frac{\dot{Q}}{A}$

where \dot{Q} is obtained from Table 5.1 for blow down process and A is the area of the detonation tube which is equal to $0.314 m^2$. The average wall temperatures produced during this process are $T_{w1} = 316.56 K$ and $T_{w2} = 300 K$.

5.2.6 Wall Temperatures During Purging Process

The wall temperatures for this process will be equal to that of the filling process as the conditions of the flow during this process are ambient and hence $T_g = T_{avg} = 300 K$. The

input parameters are $h_c = 2190 \frac{W}{m^2 K}$, $T_g = T_c = 300 K$, $t_{process} = 0.02 s$, $t_{cyc} = 0.045113 s$

and thermal conductivity k for copper at $300 K = 401 \frac{W}{m.K}$ and $\dot{q} = \frac{\dot{Q}}{A}$ where \dot{Q} is

obtained from Table 5.1 for purging and A is the area of the detonation tube which is equal to $0.314 m^2$. The wall temperatures during this process are $T_{w1} = 317.56 K$ and

$T_{w2} = 300 K$. All the averaged wall temperatures for all the processes for a detonation tube made of copper metal are tabulated.

Table 5.2 Wall Temperatures During Each Process (COPPER)

| Process | T_{w1} | T_{w2} |
|--------------------|----------|----------|
| Filling | 301.08 | 300 |
| CJ Detonation | 316.136 | 300.01 |
| Taylor Rarefaction | 316.22 | 300.01 |
| Reflection | 316.38 | 300.0 |
| Blow Down | 316.56 | 300.0 |
| Purging | 317.56 | 300.0 |

The present analysis is carried out for one cycle of operation and the values of wall temperatures from Table 5.4 clearly suggest that the temperatures of the wall vary very slowly with time due to the following conditions

1. The time taken for one cycle of operation is 0.045113 s and the time taken by the detonation process which generates the maximum heat is 0.000353 s . This suggests that the detonation time is less than 1% of the total cycle time. The remaining processes generate heat which is $1/10^{\text{th}}$ of the fraction of the heat dissipated during the detonation process.
2. The velocity of the CJ wave is $\cong 2835 \frac{m}{s}$, which suggests that the wave travels and exits the tube even before the wall material can sense a change in temperatures.

3. The cooling medium which is water in this case is assumed to be flowing through the water jacket surrounding the detonation tube at high velocities,

$$15.24 \left(\frac{m}{s} \right) \text{ and thus high value of } h_c = 2190 \frac{W}{m^2 \cdot K}.$$

4. The metal assumed in this case is copper which has high thermal conductivity of

$$400 \left(\frac{W}{m \cdot K} \right).$$

It is evident from the above cases that a temperatures change across the walls is not significant for one cycle of operation. The wall temperature responds very slowly with time and after a few cycles starts to increase linearly with time. In order to achieve greater temperature variations, the number of pulses can be incremented to a much greater value say 2000 in order to obtain a steady state solution. The averaged values of the wall temperatures for a detonation tube made up of copper and for 1 cycle of operation are $T_{w1} = 317.56 K$ and $T_{w2} = 300.01 K$.

5.3 Comparison of Copper and Steel Metals

The present analysis also aims in comparing different materials used in the construction of the detonation tube. The metal such selected should be capable of withstanding such huge temperatures that are released during the pulsed detonation cycle. In order to withstand such huge temperatures, the metal selected should have high thermal conductivity in order to allow the heat to flow through it. Hence all the above obtained values of wall temperatures for copper are compared with those of Steel (AISI304). The only difference to be made in the analysis with steel are that of the properties of steel at

300 K. The thermal conductivity of steel is $14.9 \frac{W}{m.K}$, the density $\rho = 7900 \frac{kg}{m^3}$ and

$C_p = 477 \frac{J}{kg.K}$. It is pretty evident that the wall temperatures produced while using

steel would be high when compared to copper as the thermal conductivity of steel is much lower than copper. The following table 5.5 outlines the averaged wall temperatures during each process for a detonation tube made of steel for one pulse.

Table 5.3 Wall Temperatures During Each Process (STEEL)

| Process | T_{w1} | T_{w2} |
|--------------------|----------|----------|
| Filling | 305.53 | 300.02 |
| CJ Detonation | 387.54 | 300.18 |
| Taylor Rarefaction | 388.00 | 300.19 |
| Reflection | 388.91 | 300.192 |
| Blow Down | 389.86 | 300.194 |
| Purging | 395.00 | 300.20 |

Upon comparing the values from tables 5.2 and 5.3, the wall temperatures are much higher in the case of steel for one cycle of operation. This suggests that temperatures significantly rise for steel after few cycles and hence steel cannot withstand such huge temperatures produced for longer duration of time. Hence from the above analysis, copper is preferred over steel due to its high thermal capacity which is evident from the

lower temperatures. The averaged wall temperatures in this case are $T_{w1} = 395.00 K$ and $T_{w2} = 300.20 K$.

5.4 Comparison of Transient Analysis with Steady State Analysis

5.4.1 Steady State Heat Conduction Relations

Given the nature of the pulse detonation cycle, with every process taking place in a fraction of milliseconds, there would not be any variation in the wall temperatures initially for a few cycles. However as the value of Δt is incremented i.e. there are a repetitive number of pulses taking place over a long duration of time there would be a substantial increase in the wall temperature. This process of repetitive pulses will ultimately cause high wall temperatures after a certain time period. The wall temperatures increase exponentially with time and after a certain time period become constant and do not vary with time. These temperatures are known as steady state temperatures and are obtained using the steady state conduction relations. The classical conduction solution under the steady state condition yields

$$T = T_{\infty} + \frac{\dot{Q}r_i}{k} \left[\ln(r_o / r) + \frac{k}{hr_i} \right] \quad (6.1.1)$$

After setting $r = r_i$, one obtains

$$T_i = T_{\infty} + \frac{r_i}{k} \left[\ln(r_o / r_i) + \frac{k}{hr_i} \right] \dot{Q} \quad (6.1.2)$$

This is a transcendental equation that produces T_i and then the temperature field at other locations is obtainable using the above equations as

$$\frac{T - T_{\infty}}{T_i - T_{\infty}} = \dot{Q} \frac{\ln(r_o / r) + k / (h r_i)}{\ln(r_o / r_i) + k / (h r_i)} \quad (6.1.3)$$

The state conditions exist inside the detonation tube when the time period $t \rightarrow \infty$.

Utilizing the above equation (6.1.3), the steady state values of the wall temperatures can be obtained. The average heat dissipated is calculated as follows.

$$\dot{Q}_{avg} = \frac{\dot{Q}_{fill} t_{fill} + \dot{Q}_{det} t_{det} + \dot{Q}_{taylor} t_{taylor} + \dot{Q}_{reflection} t_{reflection} + \dot{Q}_{Blowdown} t_{blowdown} + \dot{Q}_{purge} t_{purge}}{(t_{fill} + t_{det} + t_{Taylor} + t_{reflection} + t_{Blowdown} + t_{purge})}$$

Using the above value of \dot{Q}_{avg} , the wall temperatures of the detonation tube under steady state conditions are calculated using Mathematica. The temperature distribution along the inner and outer walls of the detonation tube varies asymptotically until they reach steady state values.

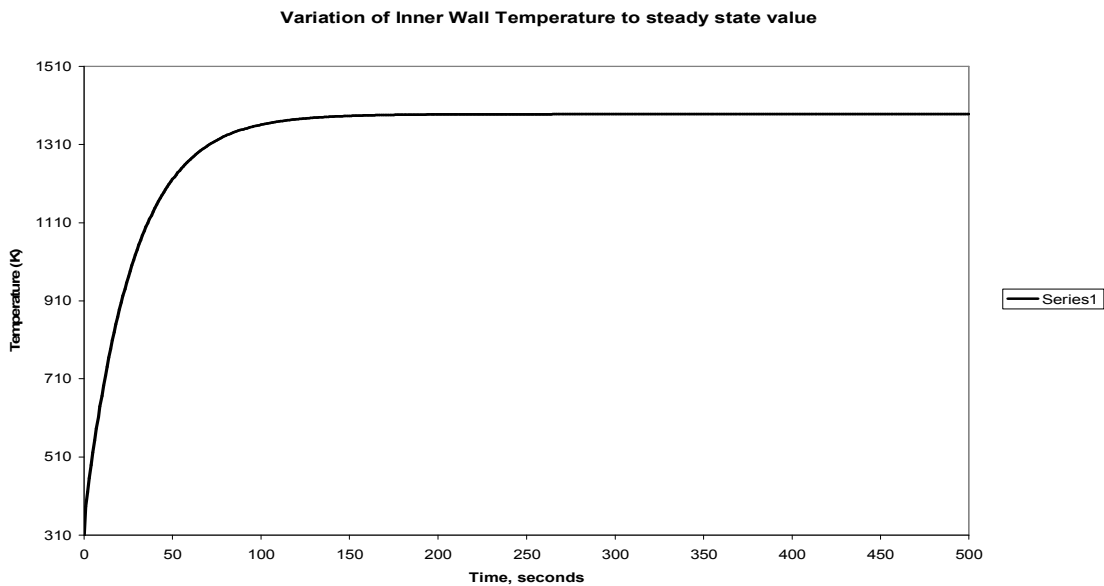


Fig 5.2 Temperature Distribution Along the Inner Walls of Detonation Tube (Copper)

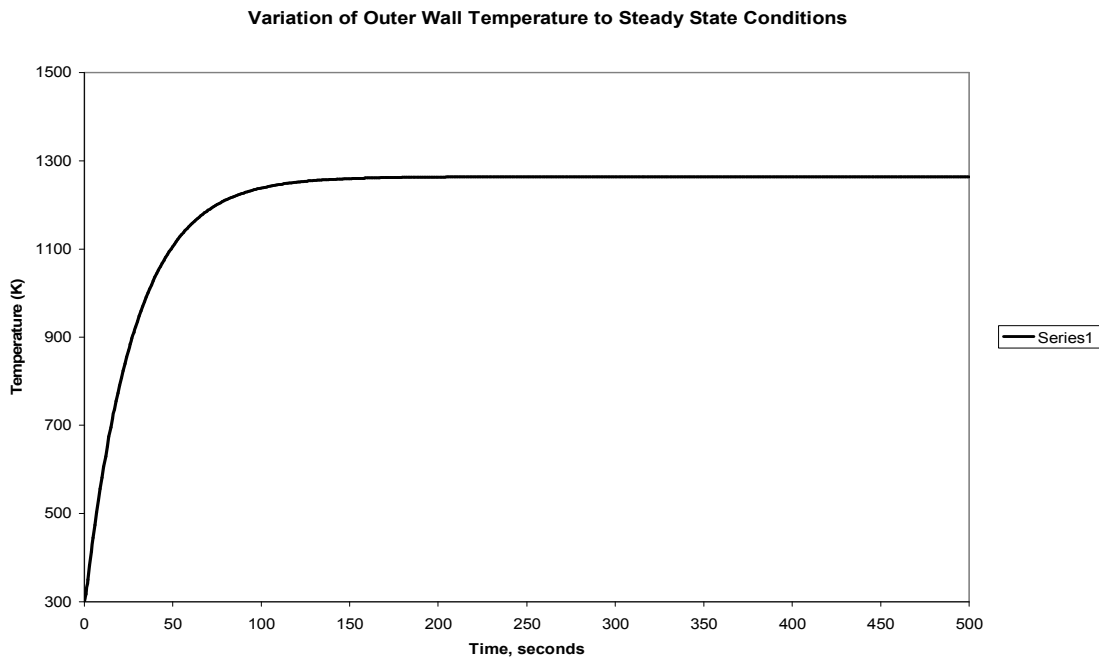


Fig 5.3 Temperature Distribution Along the Outer Walls of Detonation Tube (Copper)

It can be inferred from the above graphs that the wall temperatures initially remain ambient for a few cycles and then increase gradually until they attain steady state conditions. The wall temperatures attain steady state at about 200 seconds and remain constant after this time period. The steady state values of wall temperatures are given below.

5.4.2 Steady state values of wall Temperatures

$$T_{w1} = 1387.62 \text{ K}$$

$$T_{w2} = 1263.39 \text{ K}$$

The calculations in the transient analysis have been performed for one cycle of operation. However, as the number of cycles of operation is increased, the wall

temperatures increase gradually and reach the steady state conditions after a certain amount of time and hence it should be noted that the wall temperatures do not vary to a large extent initially. Therefore, the transient analysis solutions agree with the steady state analysis if the number of cycles is increased and also huge incremental changes in the wall temperatures take place when the heat transfer coefficient h_c is lowered to a much lesser value.

The above analysis has been repeated with steel and it has been found out that the steady state temperatures in the case of steel are of the magnitude of 4000 K which is pretty much above the melting point of steel. It is evident that steel cannot withstand such high temperatures which are generated in the walls of the detonation tube for a steel detonation tube and hence as the number of cycles of operation is increased, due to the exponential increase in the temperatures, the metal reaches its melting point thereby causing severe structural damage. Hence steel has been excluded from this analysis and only copper is considered.

CHAPTER 6

CONCLUSIONS AND RECOMMENDATIONS FOR FUTURE WORK

6.1 Conclusions

The present thermal analysis aims in developing a preliminary heat exchanger design in order to dissipate the huge amounts of heat generated from the detonation tube and to make the pulse detonation engine operational over long periods of time. The purpose of the research has been accomplished and the following parameters of the pulse detonation engine for one cycle of operation were calculated and the behavior studied.

1. The average values of Temperature, Pressure and Density for each process in the pulse detonation cycle.
2. The net heat dissipation rate of the pulse detonation engine for one cycle of operation.
3. The asymptotic approach of the wall temperatures T_{w1} and T_{w2} to the steady state conditions for a detonation tube made of copper was studied and analyzed.

All of the above mentioned parameters were calculated, by employing the unsteady state analysis and the transient heat conduction relations, the average values of temperature, the net heat dissipated and the inner and the outer wall temperatures were successfully obtained. These values were used to calculate the mass flow rate of the cooling water required to cool the tube and the initial sizing of the heat exchanger was carried out. This analysis also carries out the materials selection for the detonation tube.

and the water jacket. In this paper, steel and copper were considered and their ability to withstand huge temperatures was analyzed. Copper was ultimately chosen due to its high thermal conductivity. However, a generalized design procedure has been outlined and drafted as a Mathematica code, so that the design of the detonation tube and the heat exchanger can be varied depending on the designer's choice. The present analysis also carried out a brief study on the property distribution inside the walls of the detonation tube for one cycle of operation.

6.2 Recommendations for Future Work

The present analysis provides the following recommendations for future research.

A detailed analysis procedure has been outlined so that the design of the detonation tube and the water jacket can be modified according to designer's choice. Also a Microsoft Excel™ tool has been developed which aids in calculating the thermodynamic properties and the heat dissipated during each process for different fuel and oxidizer mixture such as nitrogen and oxygen or propane and oxygen.

The present analysis is carried out on a ground demonstrator of a pulse detonation engine. Hence water is used as a coolant in this case as ground performance parameters are independent of the weight of the engine. However, in the case of a flight demonstrator weight is the primary factor and hence in that case, the fuel itself can be used as a coolant thereby reducing the overall weight of the engine. The design procedure discussed in this analysis has the feasibility of calculating properties for any kind of coolant. Huge amounts of heat are released by ignition of the fuel oxidizer

mixture in the detonation chamber. However considerable changes in the design can be made so that the temperatures produced inside the detonation tube can be used to pre heat the fuel before it enters the detonation chamber thereby reducing the power required initially to ignite the mixture and to also improve cycle efficiency.

REFERENCES

- [1] Takuma, E. and Fujiwara, T., “A Simplified Analysis on a Pulse Detonation Engine Model,” *Trans. Japan Soc. Aero. Space Sci.* Vol. 44, No. 146, 2002.
- [2] Gordon, S. and McBride, B.J., “Computer Program for Calculation of Complex Chemical Equilibrium Compositions, Rocket Performance, Incident and Reflected Shocks, and Chapman-Jouguet Detonations,” NASA SP 273, 1976 (<http://www.grc.nasa.gov/WWW/CEAWeb/>).
- [3] Frank, P. Incropera and David, P. Dewitt., *Fundamentals of Heat and Mass Transfer*, sixth edition, John Wiley and Sons, 2006.
- [4] Mills, A F., *Basic Heat and Mass Transfer*, second edition, Prentice- Hall Inc, 1999.
- [5] Haji Sheikh, A. Beck, J V, Code, K D. and Litkouhi, B ., *Heat conduction Using Green’s Functions*, Hemisphere Publishing Corporation, 1992.
- [6] Liepmann, H.W. and Roshko, A., *Elements of Gas dynamics*, Dover Publications, Inc. Meneola, NY, 2001.
- [7] Bussing, T. and Pappas, G., “An Introduction to Pulse Detonation Engines,” AIAA 94-0263, January 1994.
- [8] J A C Kentfield., “The Thermodynamics of Air Breathing Pulse Detonation Engines,”-AIAA 01-3982, January 2001.

- [9] Kailasanath, K., "Recent Developments in the Research on Pulse Detonation Engines," AIAA Journal, Vol. 41, No. 2, 2003, pp. 145-159.
- [10] Heiser, W. and Pratt, D., *Hypersonic Airbreathing Propulsion*, AIAA, 1994.
- [11] Radulescu, M I. and Hanson, R K., "Effect of Heat Loss on Pulse Detonation Engine Flow Fields and Performance," AIAA 04-1124, January 2004.
- [12] Stuessy, W, S. and Wilson, D. R., "Influence of Nozzle Geometry on the Performance of a Pulse Detonation Engine", AIAA 97-2745, July 1997.

BIOGRAPHICAL INFORMATION

Raghu Raman Ghandikota was born in Visakhapatnam in 1985. He received his elementary education in Belmont High School. He started his Bachelors degree in Mechanical Engineering in Jawaharlal Nehru Technological University, Hyderabad in 2002 and graduated in 2006. During Undergraduation, he had undertaken internships in Hindusthan Aeronautics Limited and Visakhapatnam Steel Plant. He joined The University of Texas at Arlington in the spring of 2007 to pursue graduate studies in Aerospace Engineering. He undertook an internship at STANLEY WORKS, Dallas during the summer of 2008. His research interests include Heat Transfer, Thermodynamics apart from Computer Aided Design.